AD723319

SUMMARY REPORT

17 MAR 1971

ATMOSPHERIC PROPAGATION STUDIES

UP TO 30 SEPTEMBER 1970

D D C

MAY 17 1971

B

TELEDYNE ISOTOPES

80

IWL-7556-220

SUMMARY REPORT

17 MAR 1971

ATMOSPHERIC PROPAGATION STUDIES

UP TO 30 SEPTEMBER 1970

Hernan A. Montes

DOCUMENT CONTROL DATA - R & D

(Security classification of title, body of abstract and indexing annotation must be entered when the overall report is classified)

1. ORIGINATING ACTIVITY *(Corporate author)*	2a. REPORT SECURITY CLASSIFICATION
TELEDYNE ISOTOPES 50 Van Buren Avenue Westwood, New Jersey 07675	UNCLASSIFIED
	2b. GROUP N.A.

3. REPORT TITLE

SUMMARY REPORT - ATMOSPHERIC PROPAGATION STUDIES UP TO 30 SEPTEMBER 1970

4. DESCRIPTIVE NOTES *(Type of report and inclusive dates)*

Scientific   Final

5. AUTHOR(S) *(First name, middle initial, last name)*

Hernan A. Montes

6. REPORT DATE	7a. TOTAL NO. OF PAGES	7b. NO. OF REFS
November 1970	80	31

8a. CONTRACT OR GRANT NO. F 44620-69-C-0038 b. PROJECT NO. 9544 62701D c. d.	9a. ORIGINATOR'S REPORT NUMBER(S) IWL-7556-220 9b. OTHER REPORT NO(S) *(Any other numbers that may be assigned this report)* AFOSR-TR- 71 1207

10. DISTRIBUTION STATEMENT

This document has been approved for public release and sale; its distribution is unlimited.

11. SUPPLEMENTARY NOTES TECH OTHER	12. SPONSORING MILITARY ACTIVITY Air Force Office of Scientific Research 1400 Wilson Boulevard (SRPG) Arlington, Virginia 22209

13. ABSTRACT

A summary is given of the accomplishments of the research effort during the period 1 October 1969-30 September 1970. The phase-path (doppler) sounder array was expanded to operate at two sounding frequencies simultaneously. Particular emphasis was given to the study of ionospheric background motions having periods longer than 5 minutes or so. It was found that the power spectra of the phase-path variations show the effect of a varying Väisälä frequency with height, probably modified by the effects of viscosity. It has also pointed out the potential of the doppler technique to measure the parameters of the neutral gas structure at ionospheric altitudes. Cophase analysis of phase-path records following Saturn-Apollo launches indicate that rocket generated infrasound is trapped at ionospheric heights by a wave-guide mechanism. Ionospheric motions detected by the doppler array following a large earthquake are found to have a phase velocity equal to that of seismic Rayleigh waves of the same period and to arrive from the direction of the epicenter. A study of the spatial coherence of ionospheric motions indicates reflection point separations of the order of 60 km are sufficient for noise decorrelation up to periods of 30 min; and separations of 90 to 100 km for periods longer than 30 min. Preliminary analysis of microbarograph records following some of the French tests of 1970 show arrivals of long period gravity waves with phase velocities of the order of 550 m sec^{-1}. As part of the theoretical aspect of data processing two studies are reported.

DD FORM 1473
I NOV 55

14. KEY WORDS	LINK A		LINK B		LINK C	
	ROLE	WT	ROLE	WT	ROLE	WT
Ionospheric background motions						
Neutral structure						
Gravity waves						
Phase-path sounder array						
Array processing						
Array deconvolution						
Array response						
Spatial coherence						
Rocket generated infrasound						
Seismic atmosphere coupling						
Noise decorrelation						
Wave parameter estimation						
Atmospheric nuclear tests						

TELEDYNE ISOTOPES

ABSTRACT

A summary is given of the accomplishments of the research
effort during the period 1 October 1969 - 30 September 1970. The
phase-path (doppler) sounder array was expanded to operate at two
sounding frequencies simultaneously. Particular emphasis was given
to the study of ionospheric background motions having periods longer
than 5 minutes or so. It was found that the power spectra of the
phase-path variations show the effect of a varying Väisälä frequency
with height, probably modified by the effects of viscosity. It has
also pointed out the potential of the doppler technique to measure
the parameters of the neutral gas structure at ionospheric altitudes.
Cophase analysis of phase-path records following Saturn-Apollo launches
indicate that rocket generated infrasound is trapped at ionospheric
heights by a wave-guide mechanism. Ionospheric motions detected by the
doppler array following a large earthquake are found to have a phase
velocity equal to that of seismic Rayleigh waves of the same period and
to arrive from the direction of the epicenter. A study of the spatial
coherence of ionospheric motions indicates reflection point separations
of the order of 60 km are sufficient for noise decorrelation up to
periods of 30 min; and separations of 90 to 100 km for periods longer
than 30 min. Preliminary analysis of microbarograph records following
some of the French tests of 1970 show arrivals of long period gravity
waves with phase velocities of the order of 550 m/sec^{-1}. As part of
the theoretical aspect of data processing two studies are reported.

**TELEDYNE
ISOTOPES**

1. INTRODUCTION

Since 1968 Teledyne Isotopes has operated an array of atmospheric sensors in the New York - New Jersey area as a geoacoustic research project for the Advanced Research Projects Agency in furtherance of their nuclear test detection program. This array is unique not only in concept but in its accumulation of data derived from related phenomena in the atmosphere. Although the dominant emphasis, and recent major advance, has been in the phase-path (doppler) sounder array, the superposition of both microbarographs and magnetometers has given added support in the interpretation of atmospheric and ionospheric data. Careful planning and control in the data acquisition program has produced a high quality collection of digitized data. This has permitted us to perform analyses utilizing a number of processing schemes and computer programs in various meaningful ways. The digital data accumulated amounts to 100,000 feet of magnetic tape corresponding to more than 70 weeks of array data.

The phase-path sounder array has been expanded to operate at two sounding frequencies allowing in this way to monitor two ionospheric levels simultaneously. Array response calculations have been made to find the array's amplitude response function for various wavelengths.

The study of ionospheric background motions initiated during the previous contract year has been continued producing very important results relevant to upper atmospheric neutral structure.

Event related phenomena have been observed in connection with Saturn-Apollo launches. A preliminary dispersion analysis of the signals detected by the phase-path sounder (doppler) array has been carried out.

Ionospheric motions following the Peruvian earthquake of 31 May, 1970, were detected by the doppler array making it possible for the first time to obtain the wave parameters for this type of phenomena.

TELEDYNE ISOTOPES

As part of the array design program, a study of the spatial-coherence of ionospheric motions was undertaken. This study includes both signals and background field.

The results of preliminary analyses of microbarograph records, following the atmospheric nuclear tests at Mururoa Atoll during 1970, are reported. The analysis of the corresponding phase-path sounder records has been postponed because the conventional ionosonde data needed for their correct interpretation were not available at the time of writing this report.

Finally, in the data processing field, Dr. Eric S. Posmentier has developed a procedure for deconvolution of the array and Dr. Melvin J. Hinich has made a theoretical study of the parameter estimation of an R-dimensional plane wave which is relevant to the doppler observations.
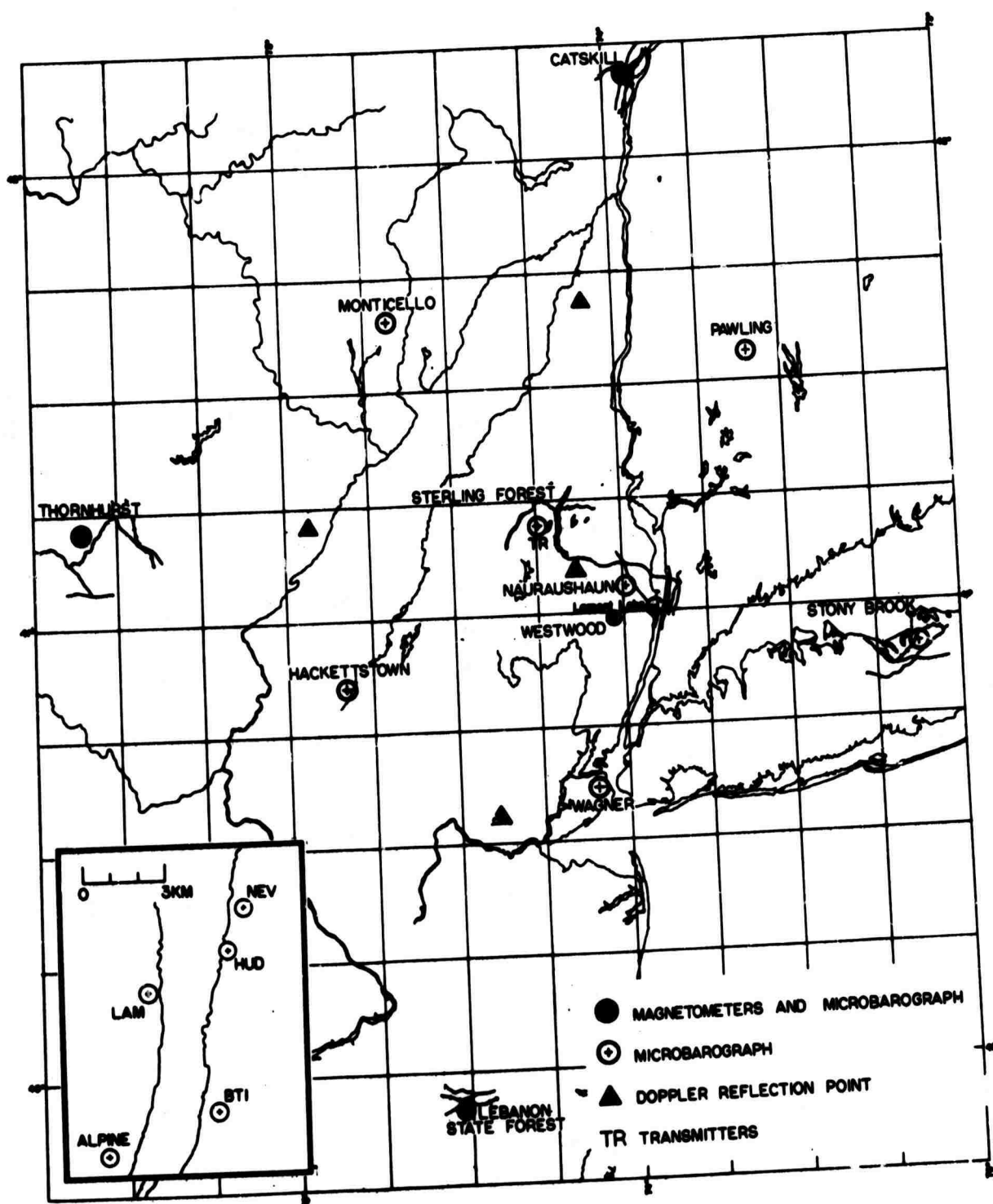
Fig. 1. Map showing the geographic distribution of the stations of the Teledyne Isotopes array.

2.1 Array Operation

During this contract year, the phase-path sounder array (Figure 1) was expanded to operate at two sounding frequencies, using the same station locations of the single frequency array. This type of operation has permitted to monitor phase-path changes at two ionospheric levels corresponding to the two sounding frequencies, 4.824 MHz and 6.030 MHz allocated by the FCC. These radio reflection levels range from 150 to 300 km depending on time of day and season.

The two-frequency array started to operate on April 1970 and has operated continuously through September 30, 1970.

2.2 Doppler System Calibration

The doppler systems used in the array were calibrated, prior to their installation at the various locations, by comparing them to a "standard system". The "standard system" was the system at Westwood. The comparison was made by applying cross-spectral analyses to the records obtained simultaneously by both systems (the one under test and the standard one). The recording interval for these tests was always greater than 12 hours, thus it was possible to compare frequency responses up to 0.5 CPH (periods of 2 hrs.). Adjustments were made until the coherence between the recordings was unity or very close to unity for all frequencies of interest.

2.3 Array Response

Array response calculations were undertaken in order to find the theoretical response of the phase-path sounder array. Plane waves, having wavelengths of 40 km to 480 km, and arrival azimuths of 0°, 90°, 180° and 270°, were assumed for these calculations. The method used in these calculations was described in an earlier report (Montes et al.,1970). Figures 2 through 7 show

CH 2, 3, 4, 5

40 KM

☐ 4 ELEMENT PHASE PATH SOUNDER ARRAY

0°

CH 2, 3, 4, 5

40 KM

☐ 4 ELEMENT PHASE PATH SOUNDER ARRAY

90°

CH 2, 3, 4, 5

40 KM

☐ 4 ELEMENT PHASE PATH SOUNDER ARRAY

180°

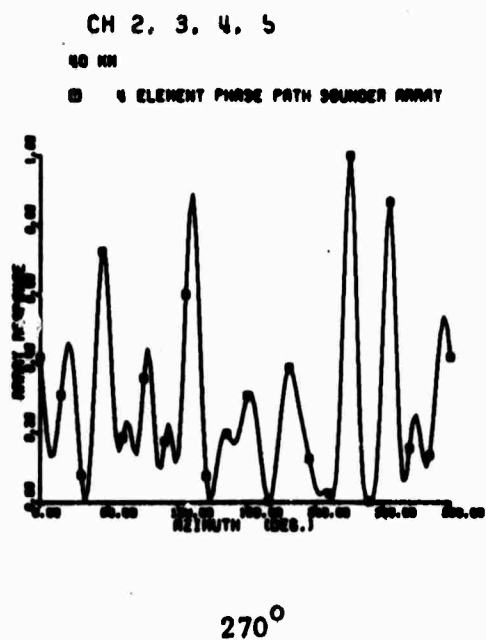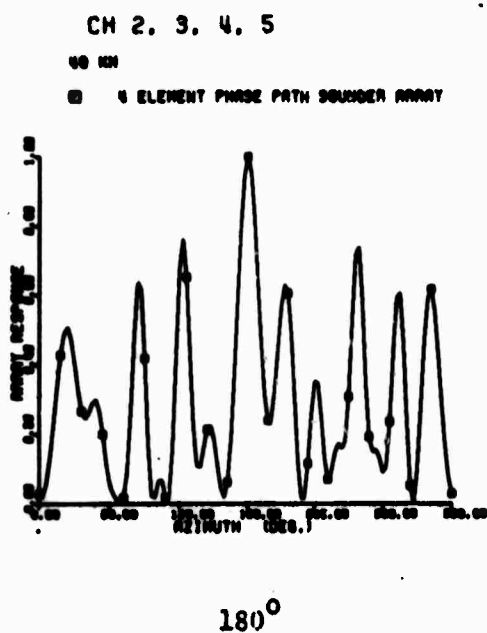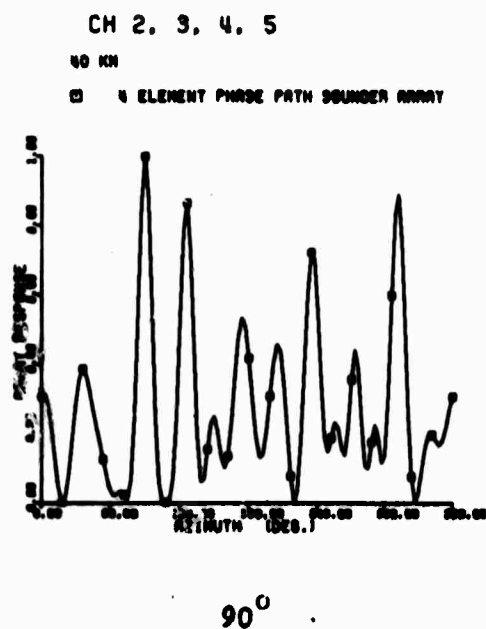CH 2, 3, 4, 5

40 KM

☐ 4 ELEMENT PHASE PATH SOUNDER ARRAY

270°

Fig. 2   Amplitude array response function for 40 km wavelength.

CH 2, 3, 4, 5

80 KM

☐ 4 ELEMENT PHASE PATH SOUNDER ARRAY

0°

CH 2, 3, 4, 5

80 KM

☐ 4 ELEMENT PHASE PATH SOUNDER ARRAY

90°

CH 2, 3, 4, 5

80 KM

☐ 4 ELEMENT PHASE PATH SOUNDER ARRAY

180°

CH 2, 3, 4, 5

80 KM

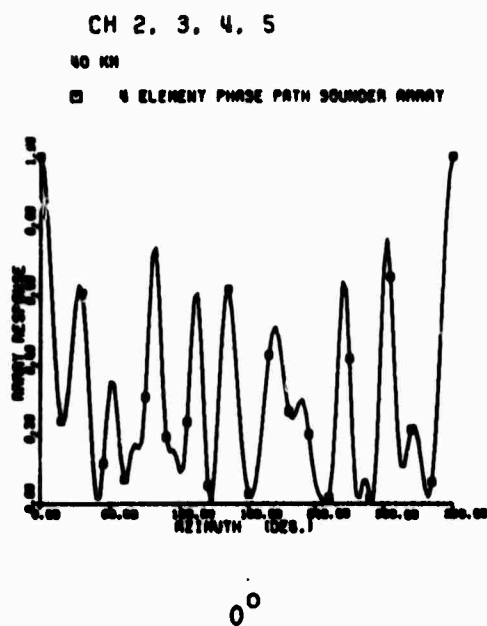☐ 4 ELEMENT PHASE PATH SOUNDER ARRAY

270°
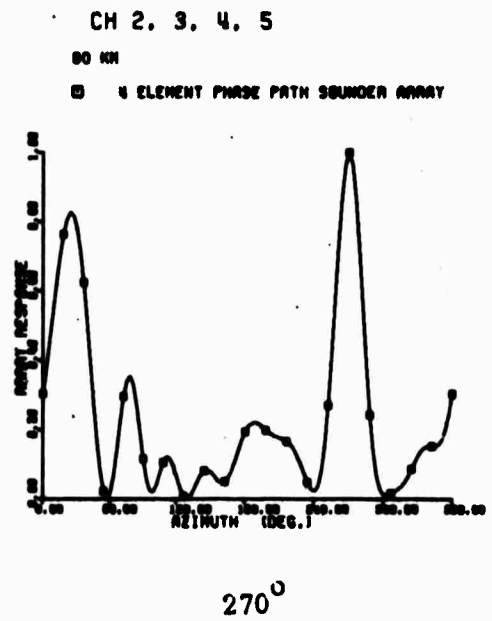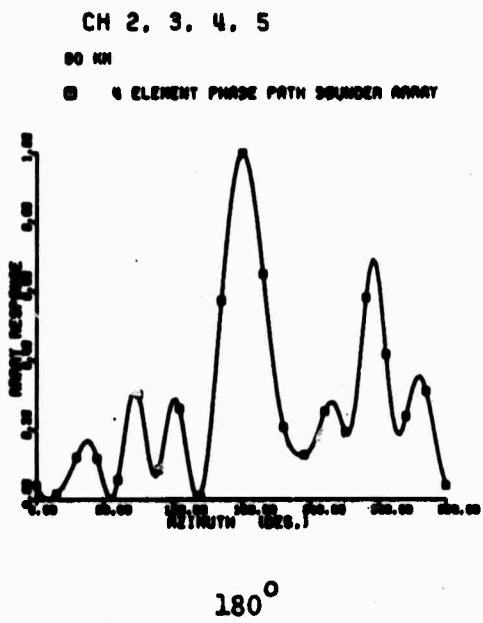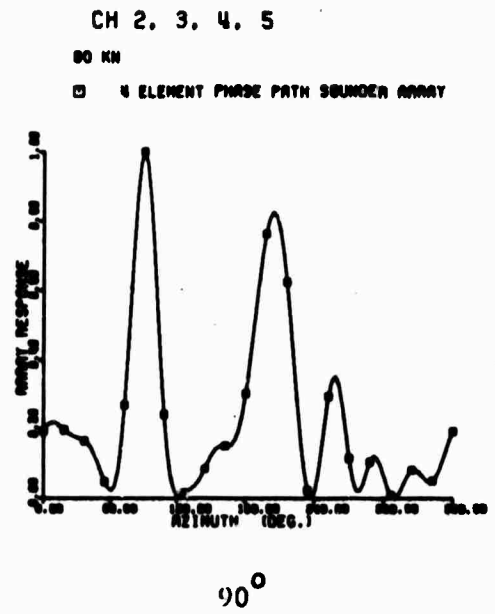
Fig. 3   Amplitude array response function for 80 km wavelength.

CH 2, 3, 4, 5

120 KM

☐   4 ELEMENT PHASE PATH SOUNDER ARRAY

0°

CH 2, 3, 4, 5

120 KM

☐   4 ELEMENT PHASE PATH SOUNDER ARRAY

90°

CH 2, 3, 4, 5

120 KM

☐   4 ELEMENT PHASE PATH SOUNDER ARRAY

180°

CH 2, 3, 4, 5

120 KM

☐   4 ELEMENT PHASE PATH SOUNDER ARRAY

270°

Fig. 4   Amplitude array response function for 120 km wavelength.

TELEDYNE ISOTOPES
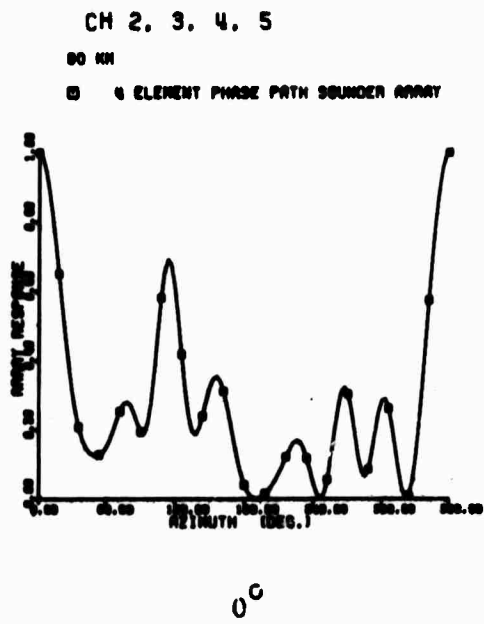
the results. It can be seen from these figures that for wavelengths of the order of 40 km, the array has many side lobes and that the magnitude of the side lobes decreases for signals coming from north or south. At wavelengths of 80 km some side lobes still persist, but the main lobe stands out clearly even for arrivals in the EW direction. For wavelengths of the order of 120 km, the array response has a large secondary lobe. This is probably a ringing effect in space since the station separations are about 60 km. For longer wavelengths the side lobes are very small and identification of an event does not present any problems.

2.4 Analog Transmission of Data

In order to determine the possibility of expanding the doppler array by adding more elements in the locations of the present microbarograph stations, some tests were carried out to see if any problems would arise when the doppler signal was transmitted in analog form from the recording station to Westwood to be digitized. Doppler analog signals were sent from Westwood to some of the existing microbarograph stations and returned to Westwood, where both the outgoing and the returned signals were digitized by the data acquisition system. Cross-spectral analyses were applied to both the outgoing and returned signals in order to find out the noise level as well as phase shifts, if any, introduced by the telephone lines. The results of a series of tests indicate that no phase shifts occurred and that only a slight amount of noise was present at periods shorter than one minute.

2.5 Pennsylvania Transmitting Station

Arrangements were made with Bucknell University at Lewisburg, Pennsylvania for the installation of a second transmitter at that location

CH 2, 3, 4, 5

240 KM

☐ 4 ELEMENT PHASE PATH SOUNDER ARRAY

0°

CH 2, 3, 4, 5

240 KM

☐ 4 ELEMENT PHASE PATH SOUNDER ARRAY

90°

CH 2, 3, 4, 5

240 KM

☐ 4 ELEMENT PHASE PATH SOUNDER ARRAY

180°

CH 2, 3, 4, 5

240 KM

☐ 4 ELEMENT PHASE PATH SOUNDER ARRAY

270°
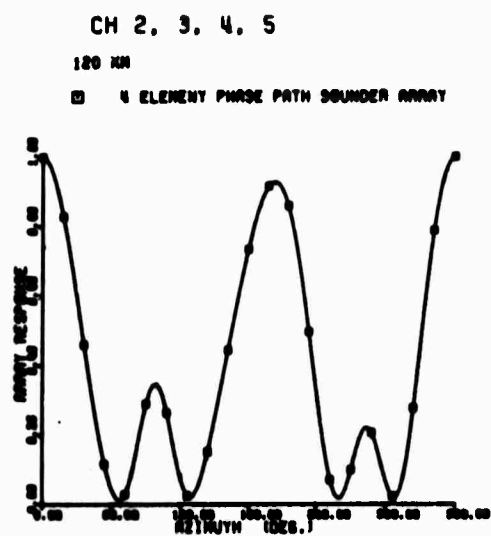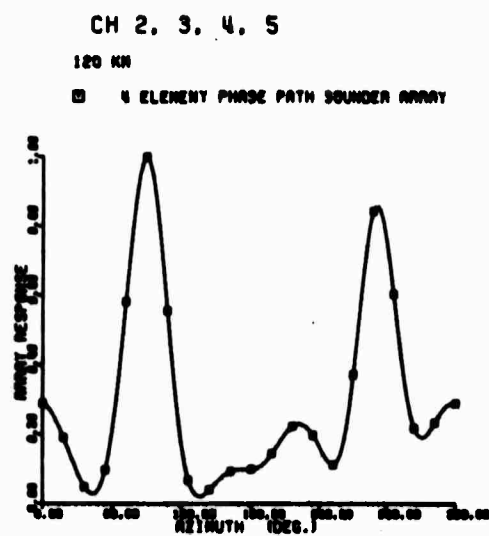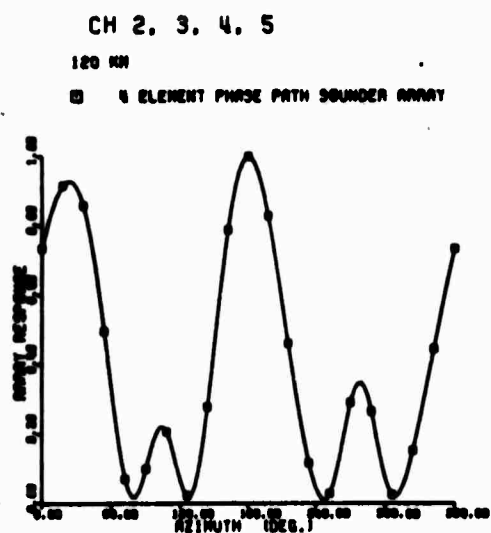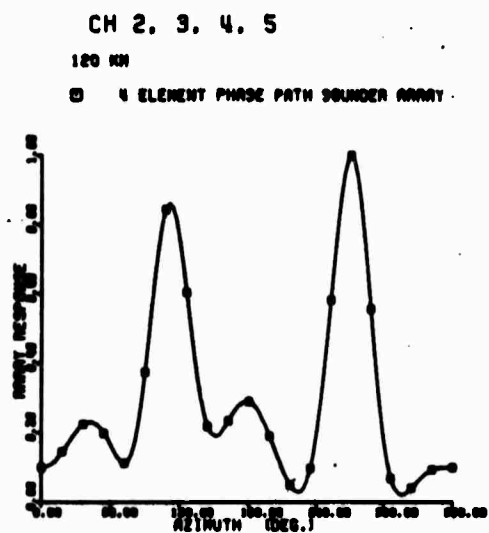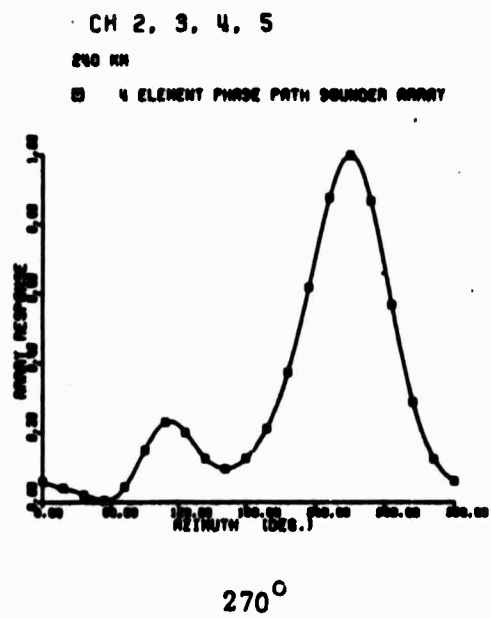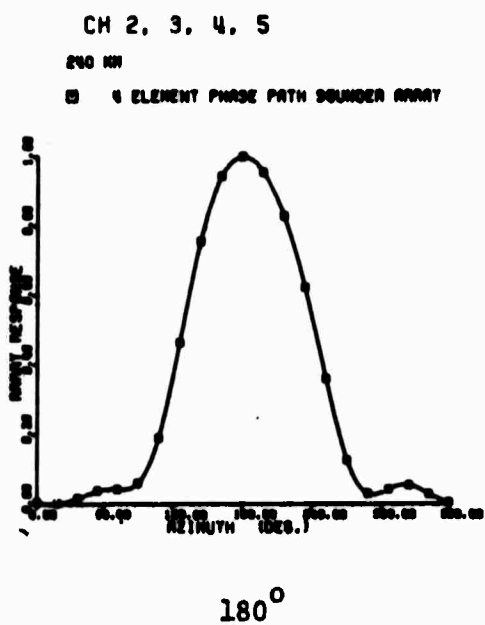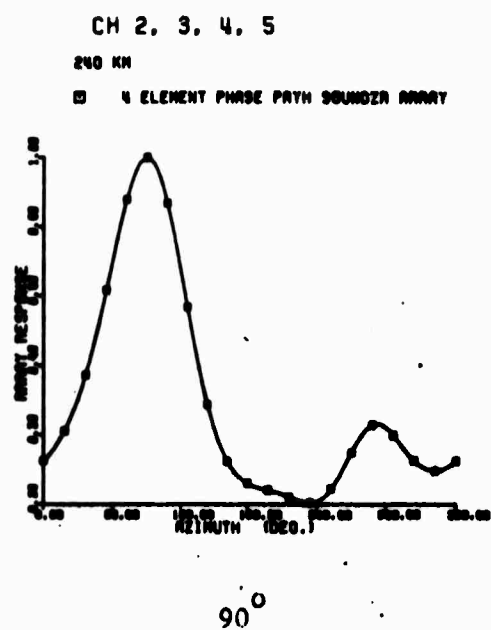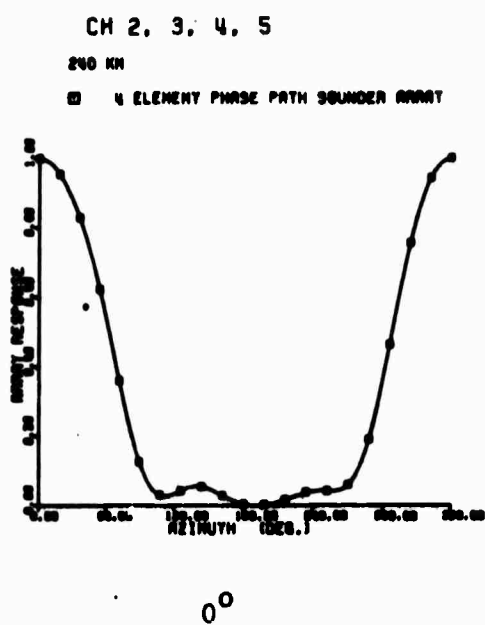
Fig. 5   Amplitude array response function for 240 km wavelength.
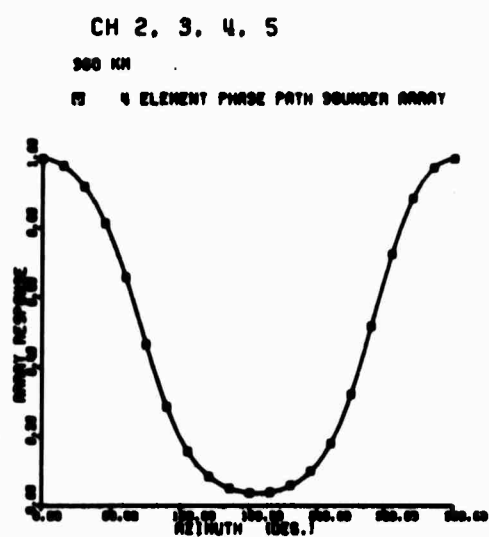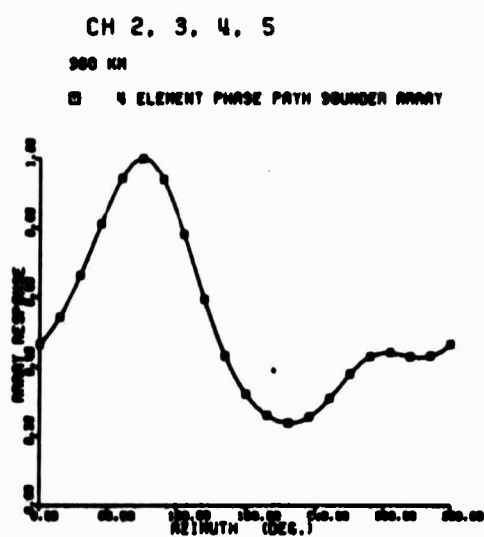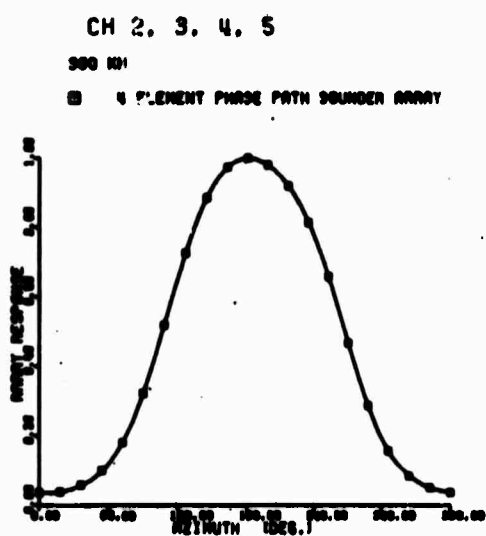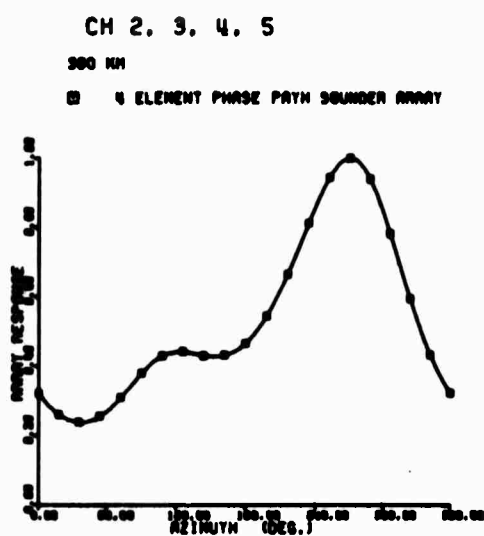
Fig. 6 Amplitude array response function for 360 km wavelength.

CH 2, 3, 4, 5

480 KM

☐   4 ELEMENT PHASE PATH SOUNDER ARRAY

0°

CH 2, 3, 4, 5

480 KM

☐   4 ELEMENT PHASE PATH SOUNDER ARRAY

90°

CH 2, 3, 4, 5

480 KM

☐   4 ELEMENT PHASE PATH SOUNDER ARRAY

180°

CH 2, 3, 4, 5

480 KM

☐   4 ELEMENT PHASE PATH SOUNDER ARRAY
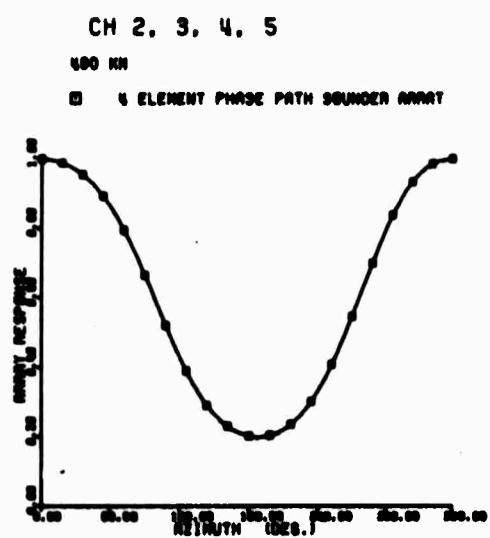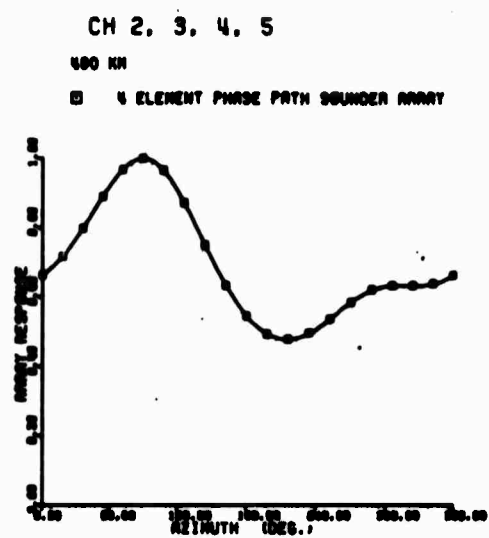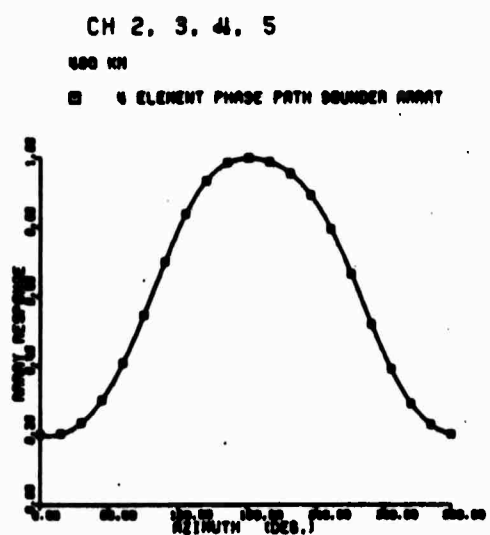
270°

Fig. 7   Amplitude array response function for 480 km wavelength.

as outlined in the proposal. The purpose of this new station was to enlarge
the aperture of the array in the EW direction and improve its resolution for
signals coming from that direction. Although most of the logistics work
had been done, the FCC did not issue the required transmitting license and
therefore this station never became operational.

A study of ionospheric background motions, using multiple-sounding frequency observations, was carried out as a joint effort with Dr. Ivan Tolstoy. A paper summarizing these results will be published shortly in the Journal of Atmospheric and Terrestrial Physics under the name "Phase Height Fluctuations in the Ionosphere Between 130 and 250 km". A more detailed version of this study is given below. The experimental set up for these measurements was reported earlier (Montes et al., 1970).

3.1 Data Analysis

The records used in this study were selected from about 20 days of data. It was assumed that the phase-path variations represent a quasi-stationary random process, and power spectra were computed using standard methods. A quasi-stationary random process is one whose spectral characteristics vary slowly so that the process appears stationary over the sample duration. Prior to the spectral analyses a pre-whitening filter consisting of a simple derivative was applied to the data. The minimum window size was dictated by the frequency separation required to distinguish the prominent peaks observed in a 24-hour window power spectrum. It was found that 4 to 6 hour-windows were reasonable. Sunrise and sunset have been avoided since the main objective was the study of the background.
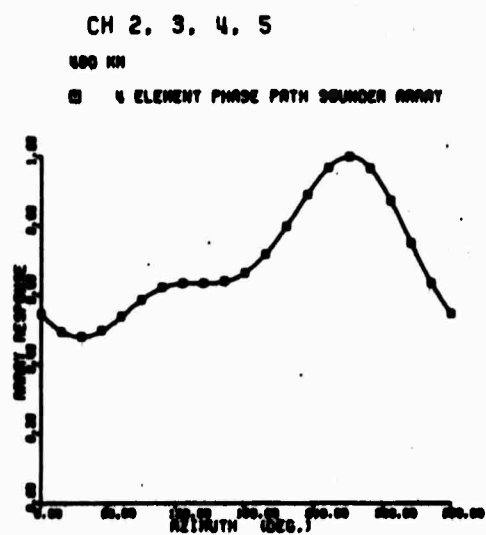
The pre-whitening filter as well as the low-pass electric filter of the data acquisition system were restored after computing the spectrum. The smoothed spectral estimates were obtained by the use of a "hanning window" and the number of lags was equal to 10% of the record length.

The power spectrum levels have been multiplied by the center frequency of the band in which the spectral estimate was calculated. Their value in the figures is in Hz^2. To convert power density levels to the amplitude of an equivalent sine wave, existing over the entire interval, which would have the

same average power, one can use the relation:

$$A(F) = \sqrt{2 \times \Delta F \times FPD/F}$$ (1)

where:

FPD = center frequency times the power density
F   = center frequency
ΔF = bandwidth.

This method of analysis has been applied to a number of records such as the ones shown in Figures 8 through 11.

3.2 Results

The power spectrum of the phase-path variations is a function of many parameters. It reflects, in particular, the spectral characteristics of the disturbance sources, the manner in which this mechanism is coupled into the medium, the efficiency of coupling to changes in the electron density, the structure of the medium, etc. In view of our almost complete ignorance concerning the mechanism by which these distrubances are generated, it is not possible to evaluate the effects of the source. In other words, a complete and truly quantitative analysis of these power spectra is not within our reach at this stage.

However, the electron motions can be computed, even if only approximately, from the motion of the neutral gas. Conversely, if the observed electron motions are due to displacements of the neutral component of the atmosphere, one may invert the procedure and deduce an order of magnitude for the motion of the neutral component from the phase path fluctuations. Thus, setting aside large hydromagnetic effects, e.g. the type associated with magnetic storms and micropulsations, and barring electron density drift of the kind occurring at sunset and sunrise, one can assume at least as a working hypothesis, that the variances
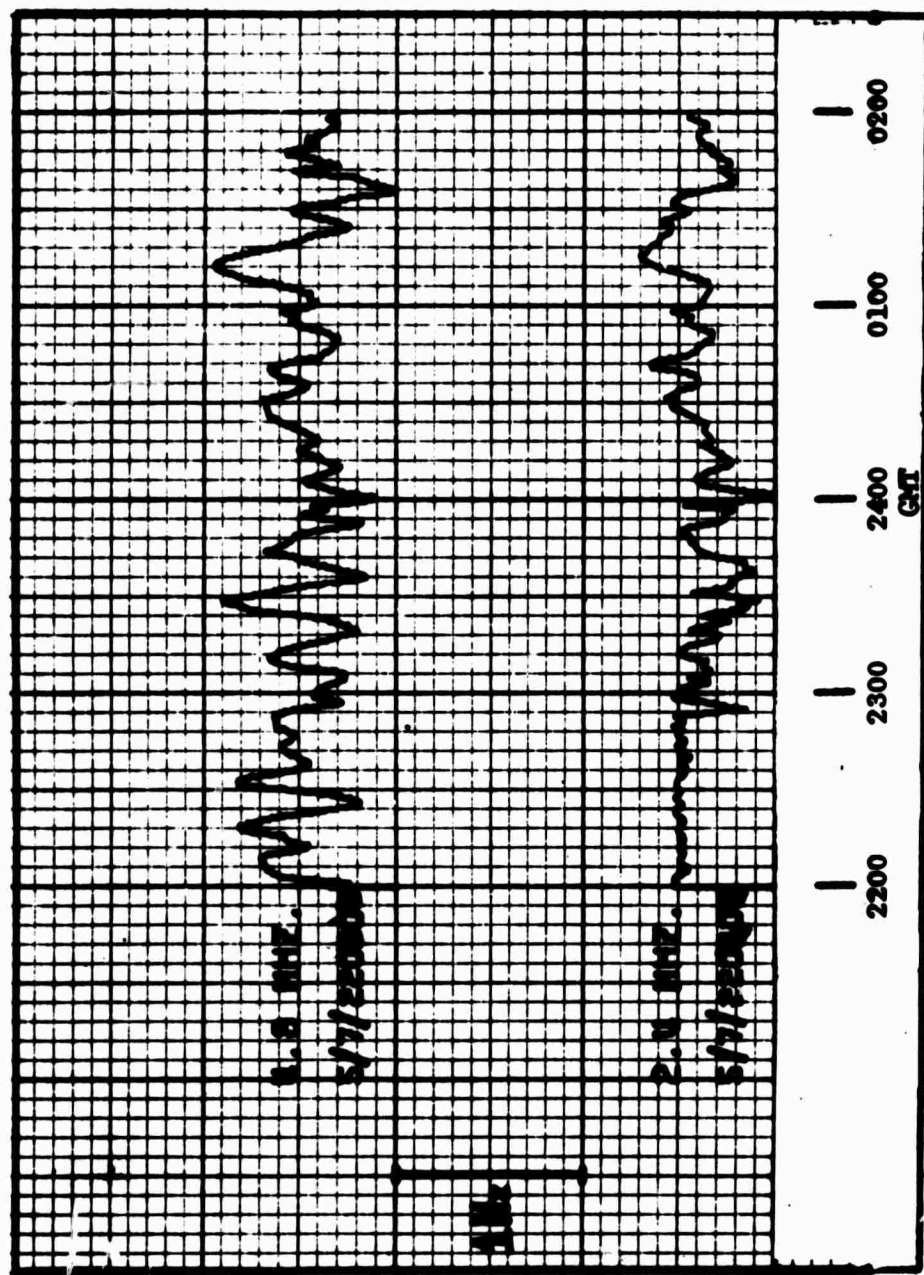
Fig. 8   Phase-path sounder traces for 2.412 MHz and 4.824 MHz on
May 7, 1969.

Fig. 9   Phase-path sounder traces for 2.412 MHz, 4.824 MHz an
6.030 MHz on June 10, 1969.

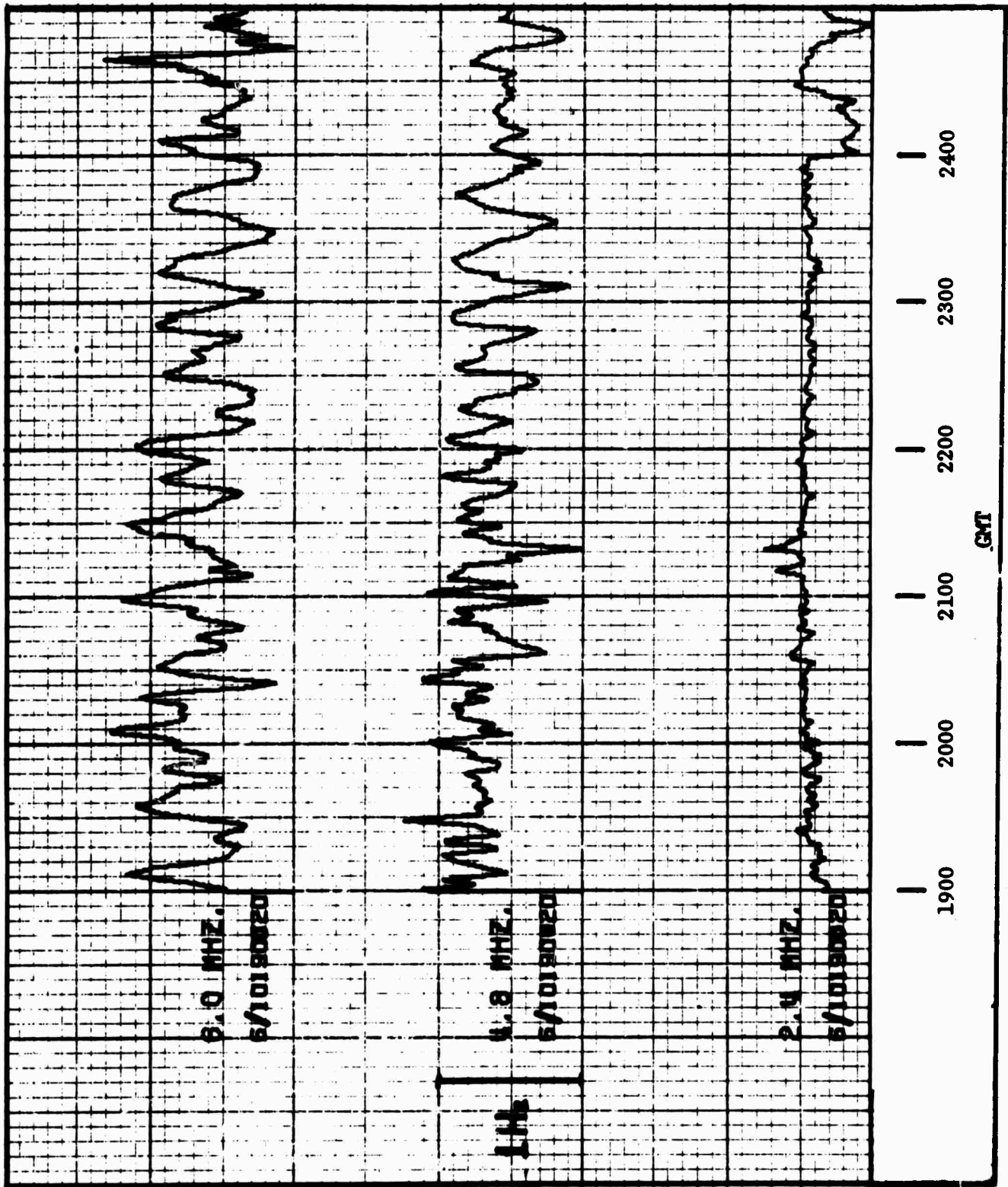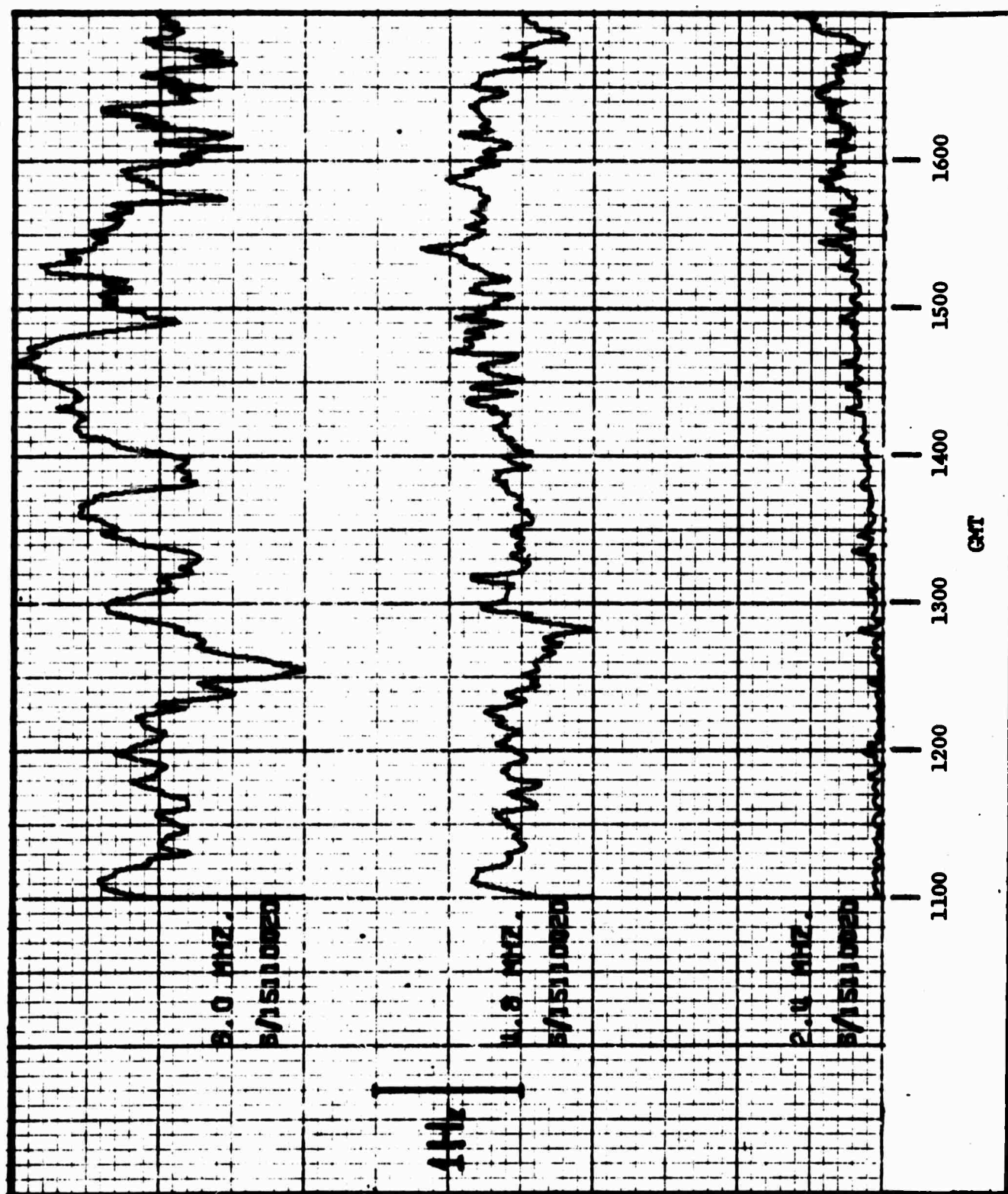
Fig. 10 Phase-path sounder traces for 2.412 MHz, 4.824 MHz and
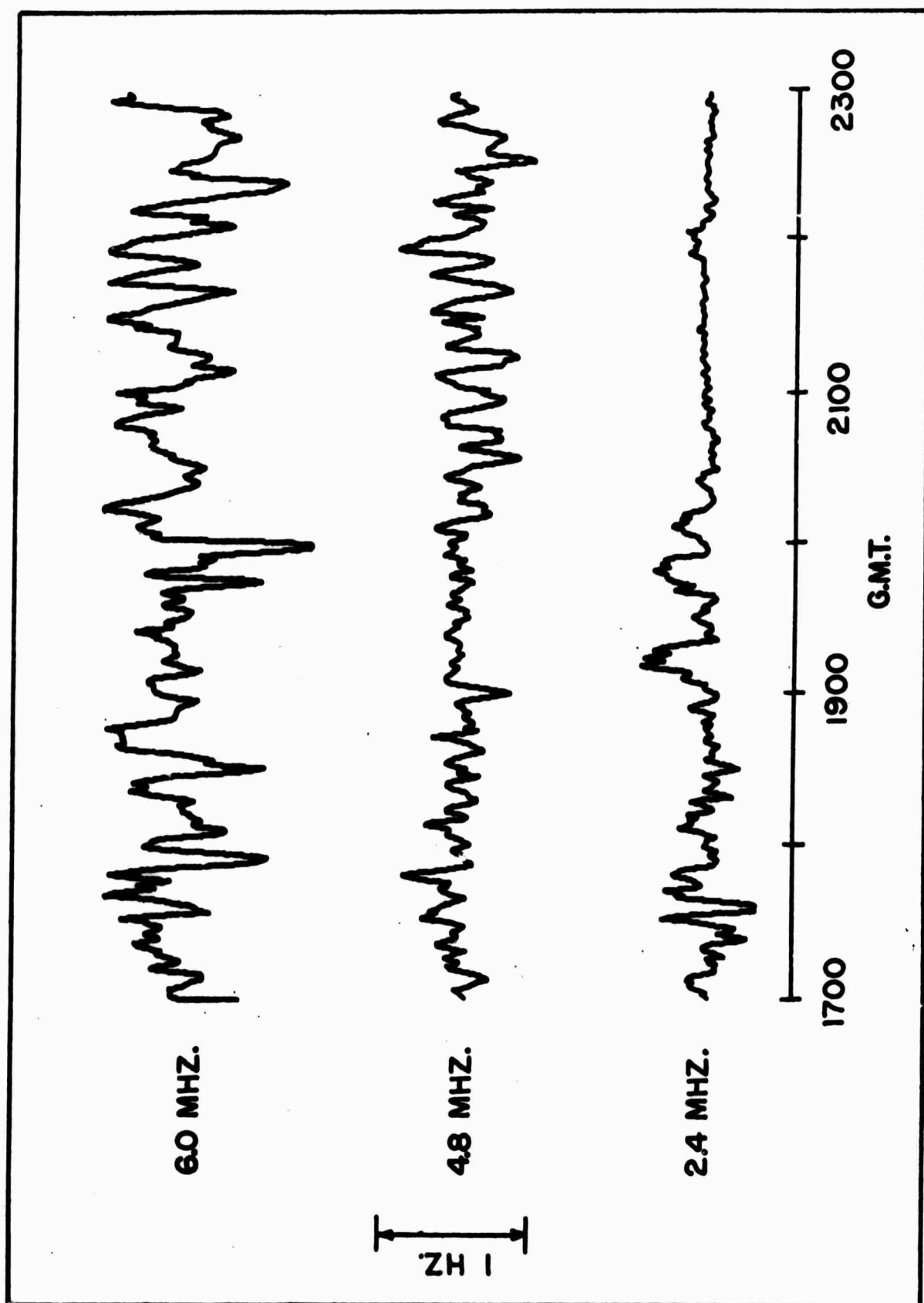6.030 MHz on June 15, 1969.

Fig. 11 Phase-path sounder traces for 2.412 MHz, 4.824 MHz and
6.030 MHz on June 9, 1969.

and power spectra shown in Figures 12 and 13 represent disturbances of both the electron and neutral components of the ionosphere. If this proposition is granted it follows that even in the absence of any knowledge concerning the origin of these disturbances, the behavior of the spectral curves can be a source of information concerning both the nature of the disturbances and the structure of the medium. Examples of the sort of thing we have in mind have been discussed in a somewhat different context in the oceanographic and meteorological literatures. For example, it has been pointed out by Phillips (1966) and Pochapsky (1968) that, given a random field of internal gravity waves, the power spectra of the wave amplitudes should show a difference in slope for frequencies above and below some locally representative value of the Väisälä frequency N. These authors have shown that observed power spectra for small motions in the interior of the ocean, plotted vs frequency or wavenumber, tend to show a steeper slope for $\omega > N$ with the break occurring near the best available estimates of N. Likewise it has been shown by Tolstoy and Herron (1969) that barographic power spectra corresponding to internal gravity waves generated by the jet-stream, show a similar pronounced change in slope occurring near an average value of N representative of the lower troposphere. This effect is due, of course, to the role of N as a high frequency cut-off for internal gravity waves (Tolstoy, 1967). However, N is also the local value of the resonant buoyancy frequency and one may expect that, under certain conditions, this frequency may show up as a maximum of the power spectrum: this should occur, in particular, for locally generated perturbations.

The power spectra shown in Figures 12 and 13 display the kind of behavior we have just discussed. There are systematic breaks in the power spectrum slopes with the shorter periods giving steeper slopes and, in a few
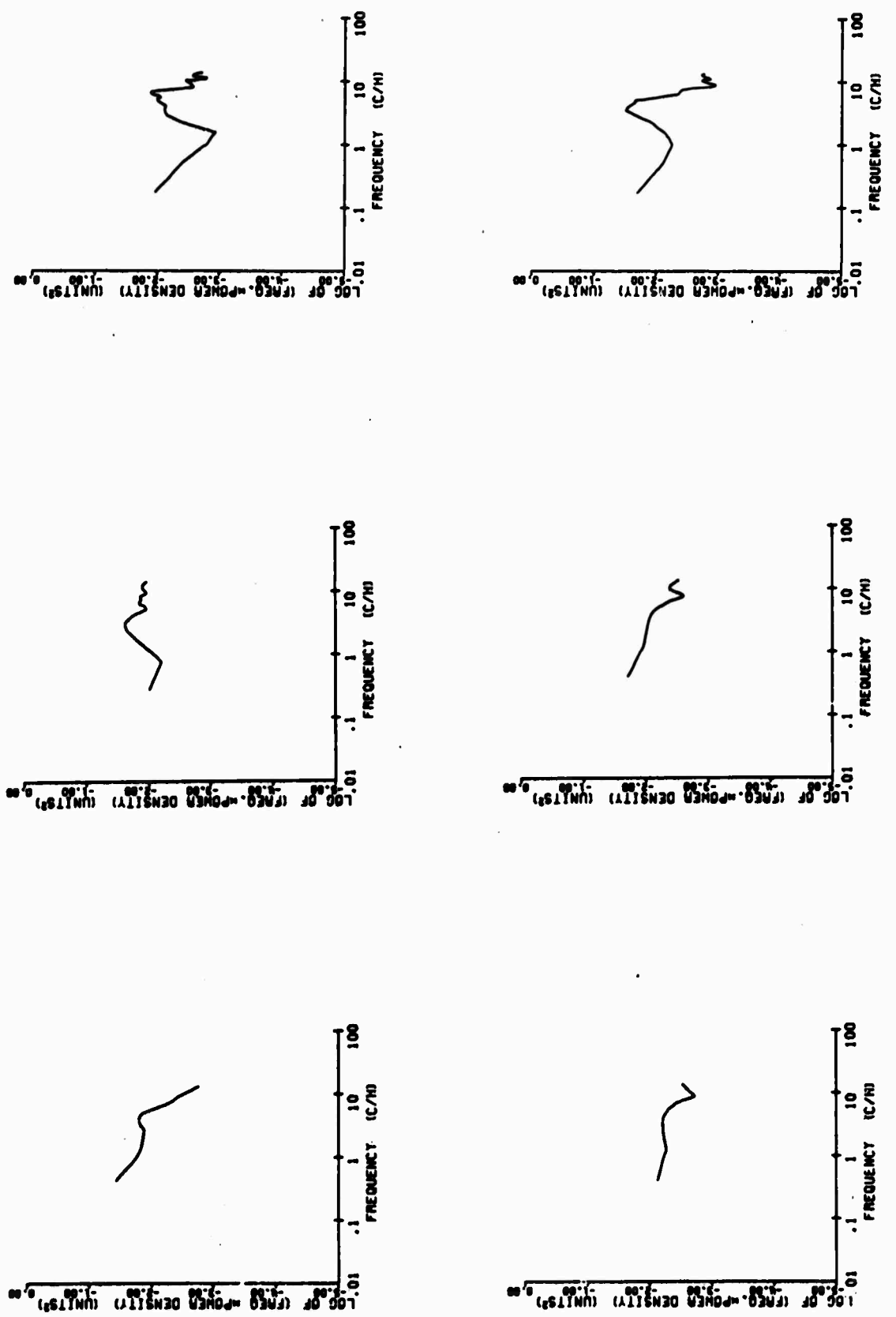
Fig. 12   Representative power spectra.
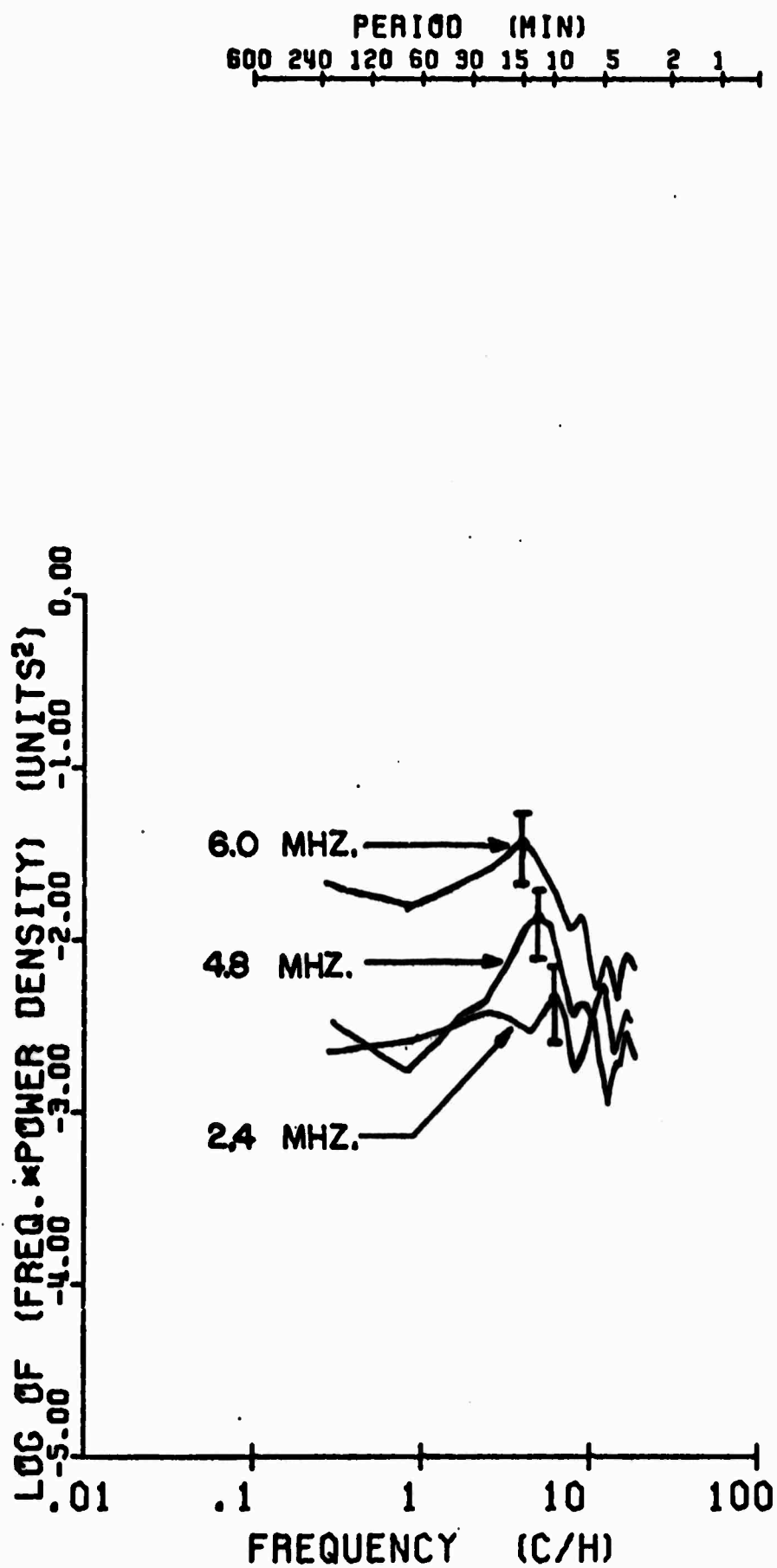
Fig. 13 Power spectrum analyses of records shown on Fig. 11,
corresponding to the time interval 1700-2300 GMT.

instances, power spectrum maxima. Furthermore, the numerical values of the breaks and of the maxima appear to shift systematically towards lower frequencies for greater radio reflection heights. Consider for example the records shown in Figure 11 which are characterized by rather obvious dominant periods. In general the amplitude and the dominant period of the trace appear to increase with increase of the sounding frequency.

Power spectral analyses confirm these observations quantitatively (Figure 13). The dominant power spectrum maxima correspond to periods between 6 minutes to 30 minutes. The magnitude of the peaks increases with sounding frequency and the periods corresponding to these peaks are distributed in such a way that shorter periods correspond to lower sounding frequencies.

The distribution of the square root of the magnitude of the peak - which is proportional to the amplitude - as function of the reflection height is shown in Figure 14. The empirical relation describing this type of distribution can be written in the form:

$$\sqrt{P} = be^{vz} \qquad (2)$$

where v is the slope of the line passing through the three points, b is a constant, and z is the height in km. Figure 14 shows that

$$v \approx 1.1 \times 10^{-5} \text{ m}^{-1}$$

The present estimate of v is a very crude one, since we have neglected to take account of possible differences with height in coupling between electron and neutral gas motion (Hooke, 1968), and since it is based on a comparison of amplitudes at different frequencies (which is only justified for a white noise source!).

The distribution of the period, corresponding to the main peak, with height (sounding frequency) shows a pattern that resmbles the distribution
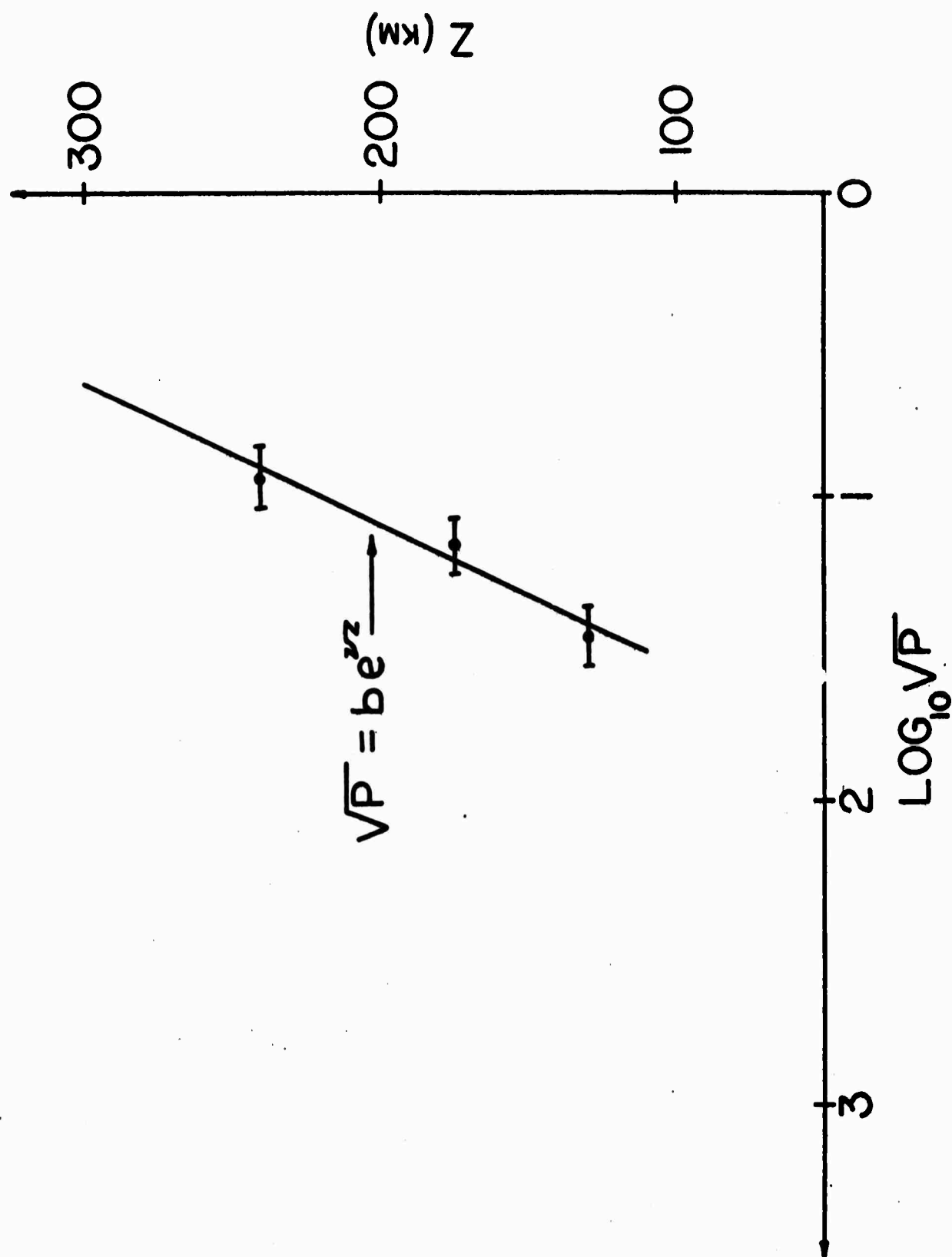
Fig. 14 Distribution of amplitude of peak periods with height,
corresponding to spectra of Fig. 13.

of the Väisälä frequency for an adiabatic atmosphere (Figure 15).

Other observations (Figure 12) show both maxima and slope changes.

3.3 Interpretation of Results

It is plausible to assume that we are dealing here with internal gravity waves. Although the precise interpretation of the curves shown in Figures 15 and 16 is perhaps open to debate and will be discussed in more detail below, there appears to be general agreement among investigators that a great deal of gravity wave activity takes place at ionospheric heights.

Observations of clearly defined wave forms in noctilucent clouds at altitudes of 90 km, suggesting horizontal gravity wave structures (Witt, 1962) and daytime and nighttime ionospheric disturbances having periods between 5 to 60 minutes (Georges, 1967; Titheridge,1968), provide important direct evidences supporting the existence of gravity wave activity at ionospheric heights.

Theoretical models describing atmospheric gravity wave propagation indicate that lower modes as well as surface gravity modes can be trapped at ionospheric heights (Tolstoy, 1967; 1970; Harkrider and Wells, 1968). Figure 17 after Harkrider and Wells shows that modes GR_o, GR_1, GR_2 for periods between 9 minutes to 30 minutes have kinetic energy maxima at heights > 110 km.

Several mechanisms for the presence of gravity waves in the upper atmosphere have been proposed. Ionospheric heating by hydromagnetic waves generated in the magnetosphere and dissipating in the ionosphere (Dessler, 1959), pulsating auroras that would provide the time varying particle flux for the generation of a pressure wave have been suggested by Maeda and Watanabe (1964), vertical energy flux from sources in the lower troposphere (Hines, 1960;

Fig. 15 Height distribution of Väisälä frequency N(z) from U.S. standard atmosphere 1966 and of observed peak frequency corresponding to spectra of Fig. 13.
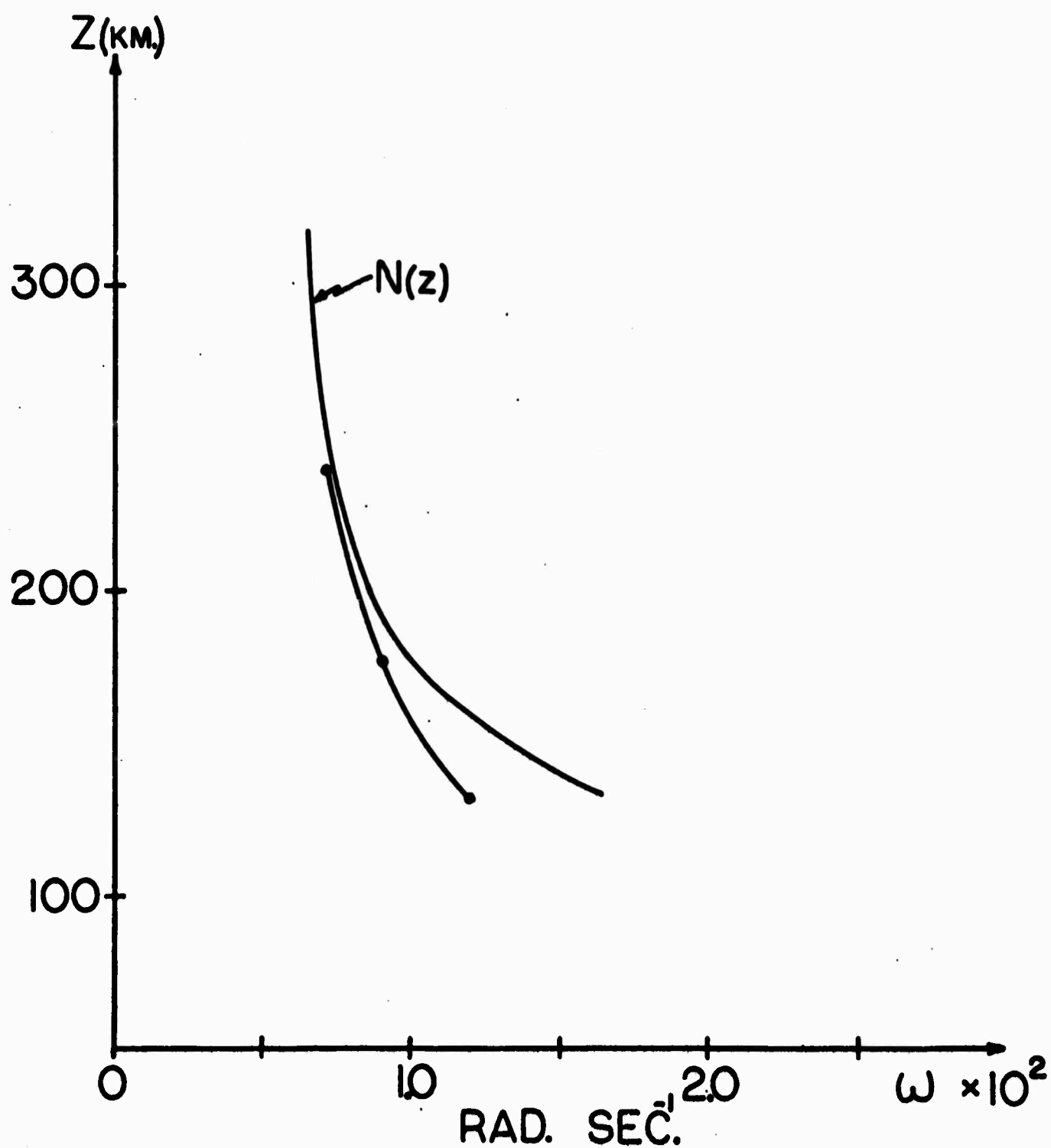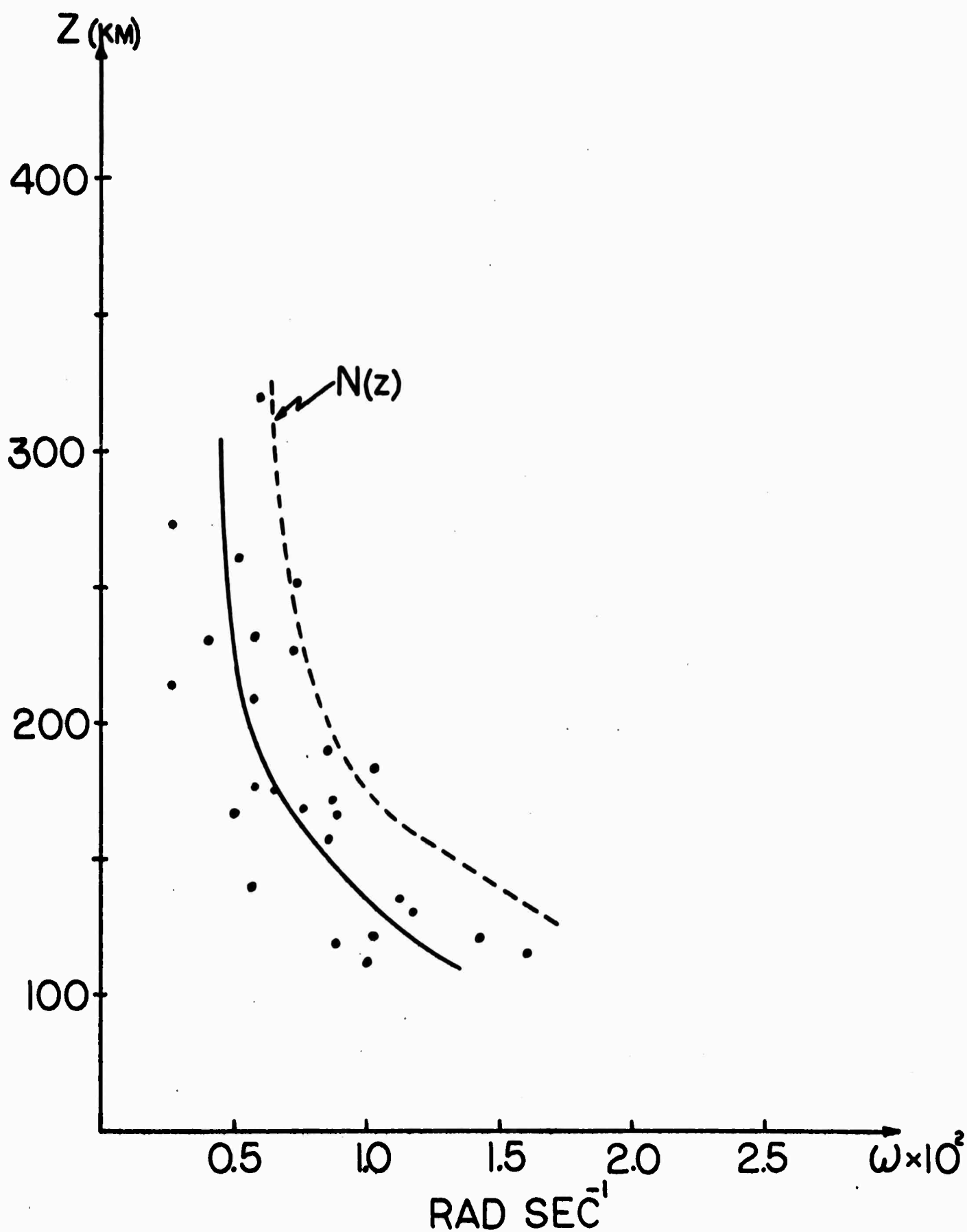
Fig. 16 Height distribution of Väisälä frequency N(z) and of peak frequency corresponding to the spectra of several records analysed.

Gossard, 1962; Mackinnon, 1967; Georges, 1968). However, there are still diffi-
culties involved in the use of many of these ideas. Thus there is the problem
of energy transfer through a critical layer. A critical layer is one in which
the wind speed equals the phase velocity of the wave. This condition may be reached
anywhere in the mesosphere or thermosphere where the wind systems attain speeds in
excess of 100 m sec^{-1}. Hines and Reddy (1967) have pointed out that transmission
of gravity wave energy can be suppressed if the wind speed opposes the phase
velocity, with such a magnitude that it doppler-shifts the wave frequencies up
to values near the Väisälä frequency below the ionosphere. Booker and Bretherton
(1967) point out a similar effect, but disagree with Hines and Reddy on the nature
of the critical layer mechanism, which they believe to be one of absorption of the
wave in the critical layer. Northward or southward propagating waves will probably
not be affected as strongly by mesospheric winds which are chiefly zonal but they
may be influenced by the winds in the lower thermosphere.

Note that equation (2) indicates an exponential dependence of amplitude
with height, of the order one would expect from a $\rho-1/2$ dependence of the kind
shown by the gravity wave amplitude predicted by elementary theory (Tolstoy, 1963).
For reasons which are obvious from an inspection of theoretical curves shown in
Figure 17, this does not necessarily provide a real measure of the local scale
height, at least not until further analysis of the energy-height curves based
upon better atmospheric models. But the result is consistent with the internal
gravity wave hypothesis.

Probably the most interesting feature of our results is the behavior
of the power spectrum peak and slope breaking frequencies with height. Our general
expectation that these are close to the local Väisälä frequency is reinforced by
the fact that plots of this frequency versus height parallel the best guess one can
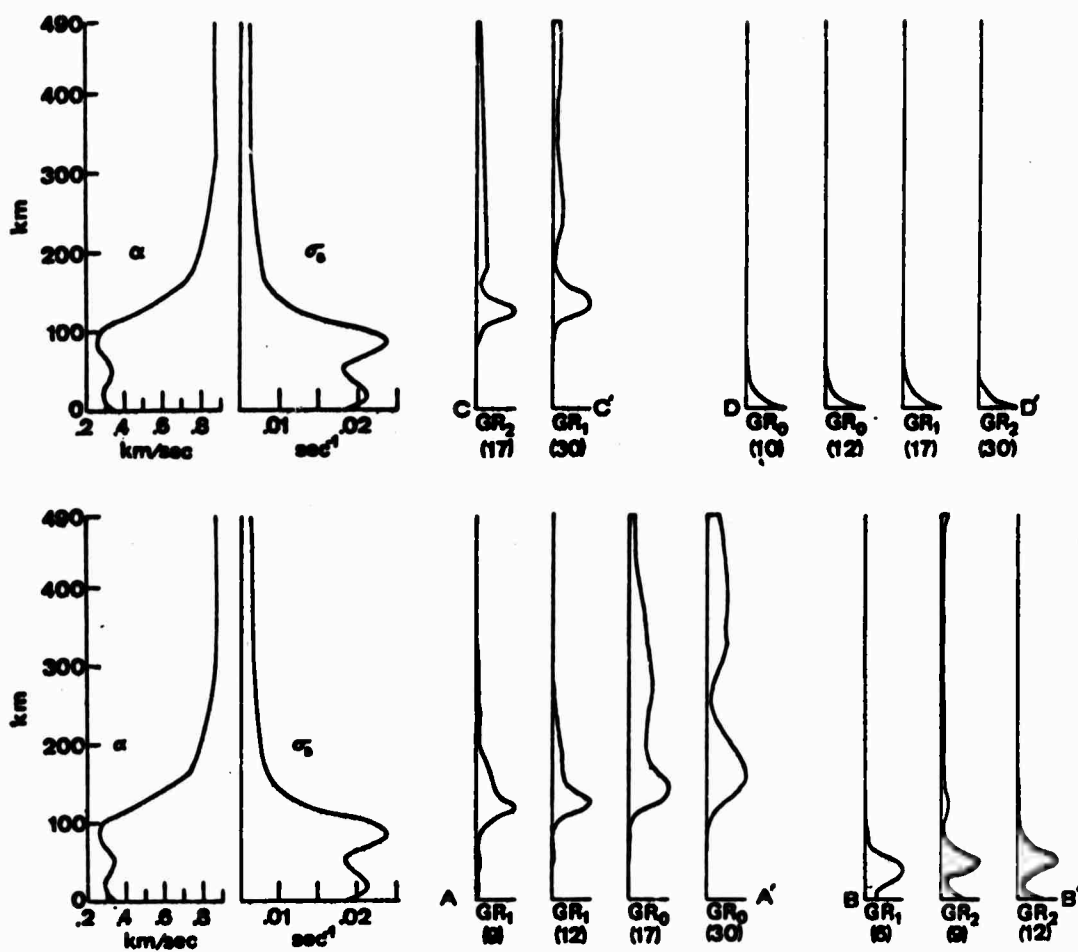
Fig. 17 Acoustic velocity, isothermal Brunt Väisälä frequency, and kinetic
energy density vs. altitude for GRo, 1.2 modes of the ARDC standard
atmosphere terminated by a free surface at 490 km.(after Harkrider
and Wells, 1968).

make for the N(z) function, based on the U.S.Standard Atmosphere Supplements, 1966. In other words, the measured frequencies of the slope breaks and peaks of the power spectrum follow the equation for N(z) given by Tolstoy (1967)

$$N(z) = \left\{ \frac{g}{T(z)} \left[\frac{g}{R^*} \left(1 - \frac{1}{\sigma} \right) + \frac{dT(z)}{dz} \right] \right\}^{1/2} \qquad (3)$$

where

g = gravity acceleration

σ = ratio of specific heats C_p/C_v

T = absolute temperature

$R^* = R/M$

with

R = universal gas constant

and

M = molecular weight,

as shown in Figures 15 and 16. This suggests that studies of this kind can be useful in determining the properties of the neutral component of the ionosphere.

The quantity N(z) is, of itself, the single most important parameter determining the behavior of internal gravity waves at these heights: this type of information is needed for interpreting the propagation behavior of TID's.

We have stressed the importance of the gravity wave concept in producing the kind of background ionospheric activity discussed in the last few sections. In the process we have pointed at the likelihood of the power spectrum slope breaks and maxima being representative of the local value of the Väisälä frequency N(z).

An alternative explanation of the behavior of these observed frequencies

with height can be suggested, involving the effects of viscosity following a line of argument suggested by Pitteway and Hines (1963) and Georges (1967). It is clear that, as ρ decreases, the importance of the viscous terms will rise in comparison with the inertial (acceleration) terms. In other words, although the molecular viscosity μ stays fairly constant, the kinematic viscosity:

$$\eta = \frac{\mu}{\rho} \tag{4}$$

increases without limit as $\rho \rightarrow o$. At heights in the 200-250 km range, one would have, according to Midgeley and Li-mohn (1966):

$$\eta \simeq 10^5 \ m^2 \ sec^{-1} \tag{5}$$

This imposes a severe limitation on the scale of the disturbances which can be expected to propagate at any frequency ω . Thus, for a given ω the wave attenuation in the horizontal direction goes like $e^{-\delta x}$, where an order of magnitude for δ is (Tolstoy, 1967):

$$\delta \simeq 2\eta \frac{Kx^2}{V_{ph}} = 2\eta \frac{Kx^3}{\omega} \tag{6}$$

where

      Kx = horizontal wave number.

This implies that for frequencies of the order of 10^{-2} rad sec^{-1} (periods of about 10 min), propagation to distances greater than a wavelength requires wavelengths in excess of 60 km, or what is equivalent, phase velocities of 100 m sec^{-1} or better. Although this is not inconsistent with observation (Georges, 1967; Titheridge, 1968), it shows that viscosity is beginning to limit severely the spectrum of allowable wavelengths.

TELEDYNE ISOTOPES

Georges (1967) has demonstrated that the spectra of 3.3 MHz phase-path fluctuations have a diurnal behavior, with peak periods of about 5 min around noontime, dropping to well below 15 min at night. Georges explains this behavior in terms of the opposing effects of viscosity and the $\rho^{-1/2}$ amplitude increase with height. Although his results are certainly consistent with such an explanation, they do not prove the hypothesis.

We believe, on the other hand, that the power spectra presented nere show the effect of a varying Väisälä frequency with height, probably modified to some extent by the effects of viscosity. As already emphasized, it is not possible to offer a quantitative theory of the power spectrum behavior, so that one cannot rule out an explanation based primarily on the role of viscosity, but the following points appear suggestive.

1) The fact that the power spectrum peaks or slope breaks tend to follow the calculated $N(z)$ curves cannot be explained solely on the basis of viscosity: in the viscosity hypothesis, this effect would appear largely as a coincidence.

2) The appearance itself of power spectrum peaks for N is difficult to explain by the effect of viscosity alone, since this would require a generating process with a spectrum having the unlikely property of rising steeply towards the shorter periods, before being knocked down and filtered out of existence by viscosity.

3) The appearance of breaks in the power spectrum slopes, of the kind shown in Figure 12 is more suggestive of a frequency cutoff effect than of a steadily increasing viscous damping.

4) George's results appear to be equally consistent with our hypothesis. In other words, his atmospheric stop-band filtering effects are also in agreement with the critical nature of the Väisälä frequency.

To conclude, therefore, it appears likely that the peak frequencies and slope break frequencies measured on the phase path fluctuation power spectra are representative of the local values of the Väisälä frequency $N(z)$. But although the coincidence of these measurements with the calculated $N(z)$ curves is striking, it remains true that any truly quantitative interpretation of the power spectra will necessitate the introduction of viscosity into the theory.

Following several Saturn-Apollo launches, the phase-path sounder array
recorded doppler frequency variations having periods of the order of a few min-
utes. Typical records corresponding to the Saturn-Apollo 12 and 13 launches are
shown in Figure 18. The signal-to-noise ratio is of the order of 1. Cophase
analyses were applied to the records of the phase-path sounder array using an
80-min time window which included the whole signal (Figs. 19 and 20). The
average phase velocities and arrival azimuths are 720 m sec^{-1} and 175° for
the Saturn-Apollo 12 and 735 m sec^{-1} and 175° for the Saturn-Apollo 13. The
direction of arrival intersects the trajectory of the rockets at 30.74°N,
72.76°W, and an altitude of 160 km . The horizontal distance between this point
and the center of the array is 1144 km, giving a group velocity of 460 m sec^{-1}.
Preliminary dispersion analyses of the signals for both events were carried out.
The results of these analyses have been published in the Journal of Geophysical
Research as a joint effort with Dr. I. Tolstoy of Florida State University
under the title: "Long Period Sound Waves in the Thermosphere from Apollo
Launches".

The observed phase and group velocities have been explained by Tolstoy
et al., (1970) as the trapping of the rocket generated acoustic waves at iono-
spheric heights by a wave-guide effect. The waves are totally reflected at the
top of the wave-guide by the increasing sound speed, and almost totally reflected
at the bottom, from the mesosphere, by the steep density gradient and consequent
increase of the acoustic cut-off frequency.

It must be pointed out that these signals have not been found on the
microbarograph records. Further investigation of the Saturn-Apollo generated
signals is under way in order to establish the circumstances under which these
signals show up in microbarographs and phase-path records. Doppler sounders and
microbarographs have been in operation during the Apollo 8 thru 13 launches.
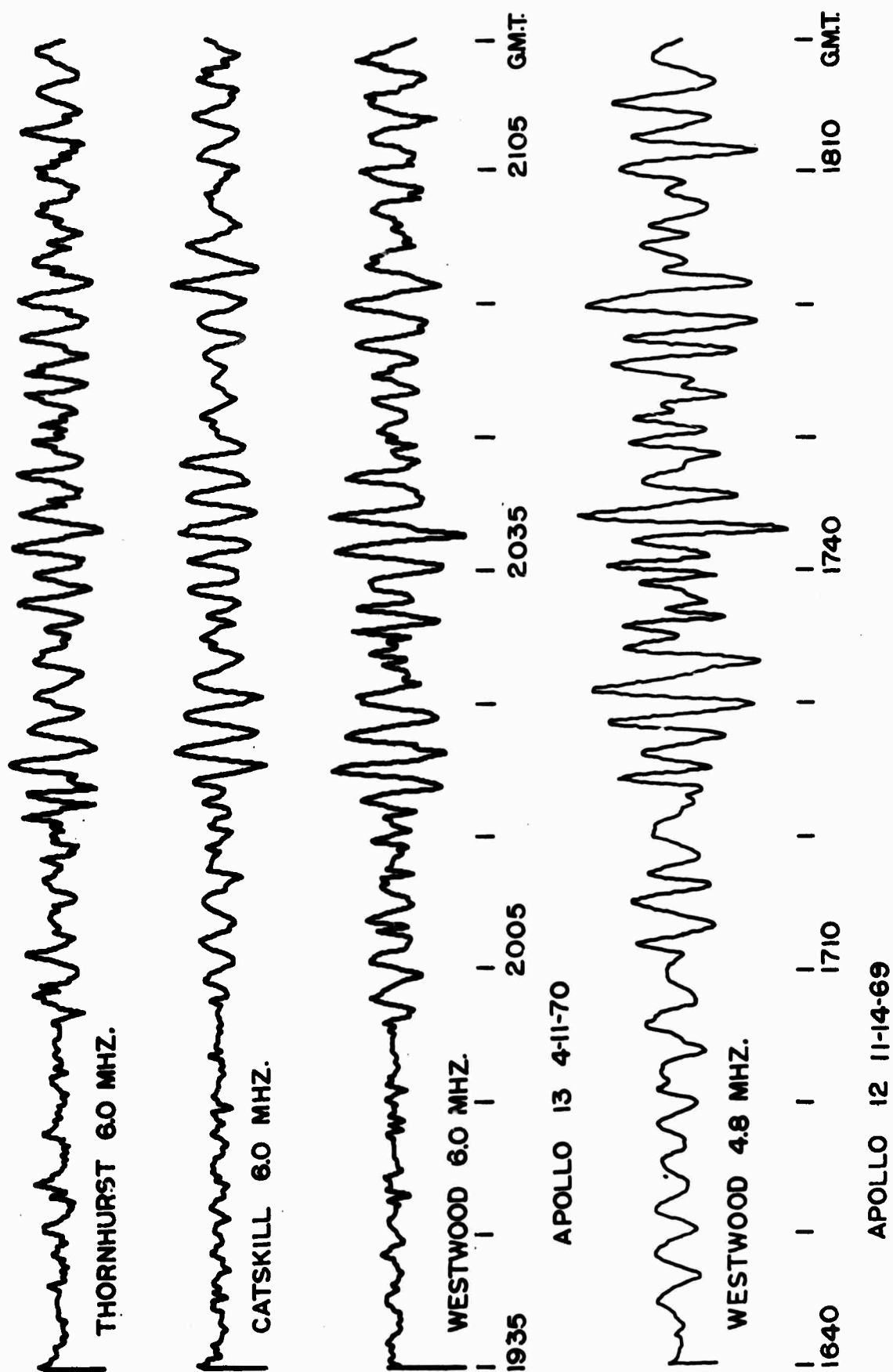
Fig. 18 1-5 min period bandpass filtered phase-path sounder recordings at several stations of array in Fig. 1 for Saturn-Apollo 12 and 13 events.

NORTH
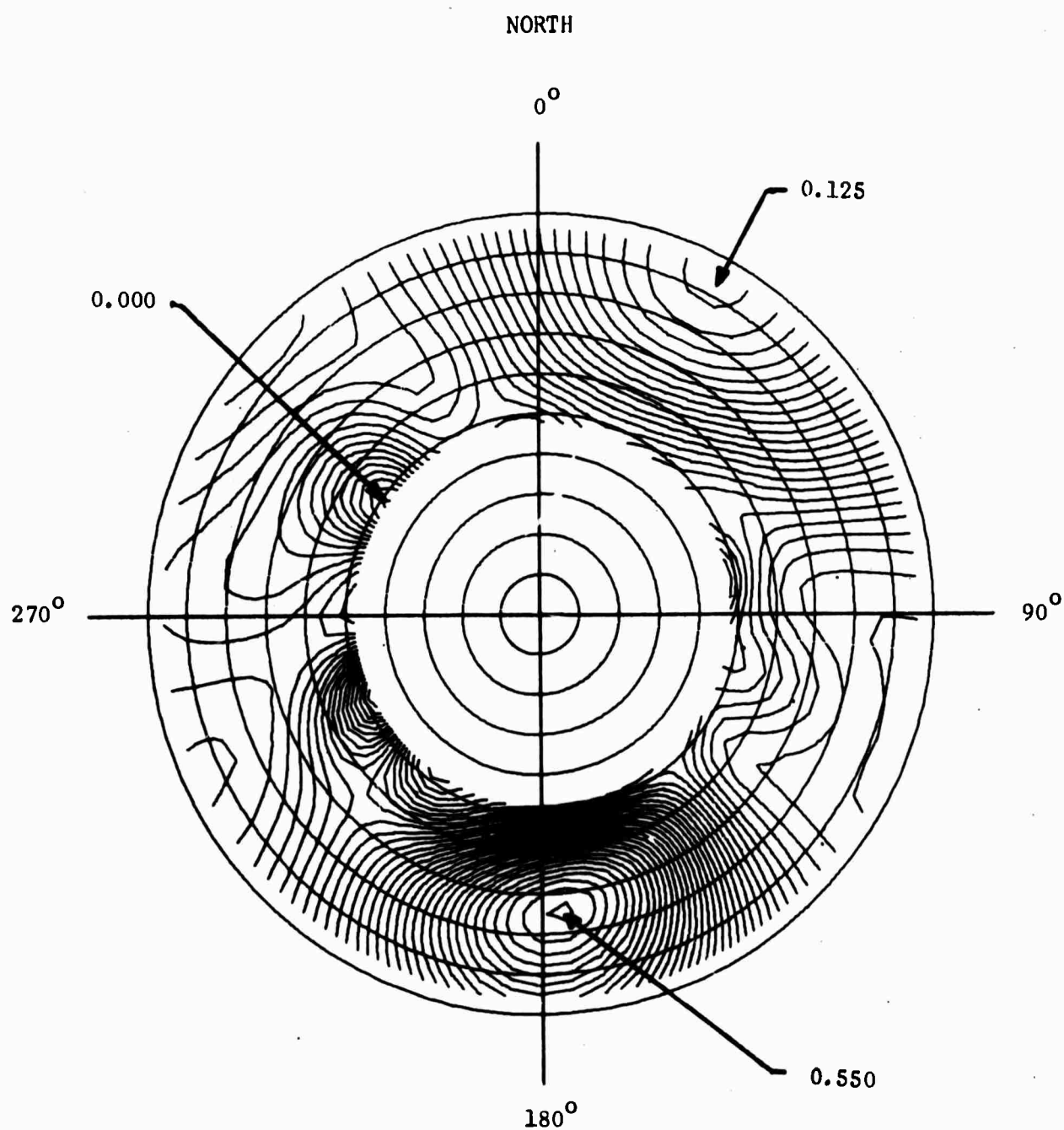
Fig. 19 Contour plot of $C(v,\theta)$ for 80 min window starting at 1710 Z on November 14, 1969. Radius is velocity, from 0 to 1000 m sec^{-1} in steps of 100 m sec^{-1}. Contour interval is 0.01.
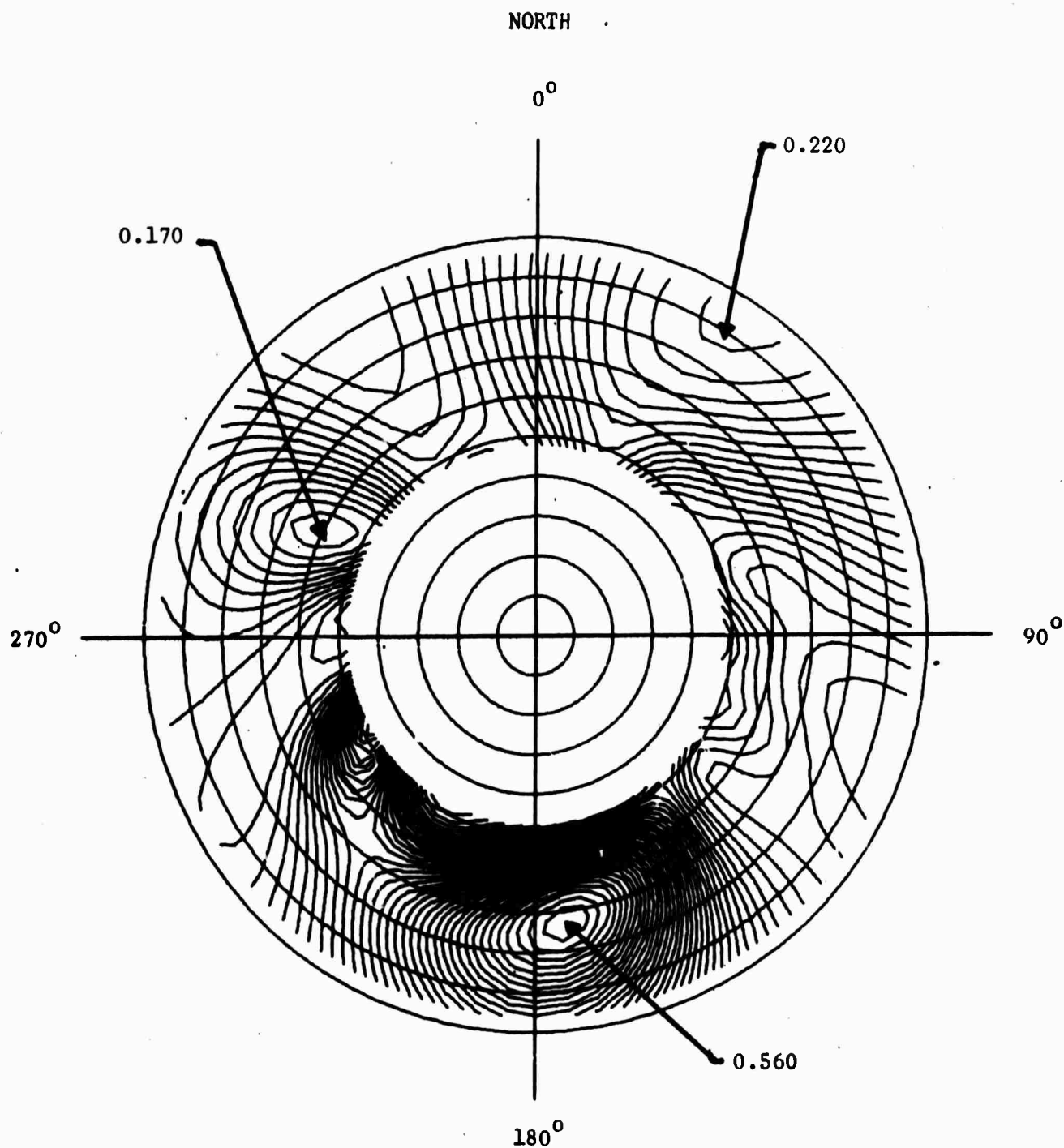
Fig. 20 Contour plot of C(v,θ) for 80 min window starting at 2000 Z on April 11, 1970. Radius is velocity, from 0 to 1000 m sec^{-1} in steps of 100 m sec^{-1}. Contour interval is 0.01.

**TELEDYNE
ISOTOPES**   5.   IONOSPHERIC MOTIONS COUPLED WITH SEISMIC RAYLEIGH WAVES

Doppler frequency variations having periods between 0.3 and 3 min and

amplitudes of about 0.4 Hz (Fig. 21) were recorded by the array of phase-path

sounders on 31 May 1970 at about 2047 GMT. Cophase analysis of the records

indicates that these signals are propagating with a horizontal phase velocity

of about 3.9 km sec^{-1} and that the azimuth of the arrival is 190° $\pm$ 5° (Fig. 22).

The time of arrival corresponds to the time of arrival of seismic Rayleigh waves

from the Peruvian earthquake of 31 May 1970. The group velocity computed from

arrival time is 3.8 km sec^{-1}. This group velocity agrees well with that of

seismic Rayleigh waves (Oliver, 1962). These arrivals can therefore be explained

as produced by the coupling of seismic Rayleigh waves into the atmosphere.

The coupling of seismic Rayleigh waves with atmospheric waves has been

discussed theoretically (Jardetsky and Press, 1952). Pressure fluctuations

observed at ground level have been interpreted as the atmospheric wave part of

this coupled mode (Donn and Posmentier, 1964). Davies and Baker (1965) and

Weaver et al. (1970) have observed ionospheric disturbances believed to be high

altitude manifestations of the same mode. All of these interpretations were

based on the agreement between seismic and atmospheric arrival times, or group

velocities.

The data presented here is the first example of the determination of

the phase velocity and direction of a seismic-coupled atmospheric wave observed

at ionospheric levels. The phase velocity of 3.9 km sec^{-1} agrees well with that

of Rayleigh waves (Oliver, 1962), and the direction of 190° $\pm$ 5° is consistent

with the azimuth of the earthquake (185°). These comparisons are two of the

most important evidences of coupling between seismic surface waves and atmospheric

waves. It must be added that the analysis of the microbarograph records
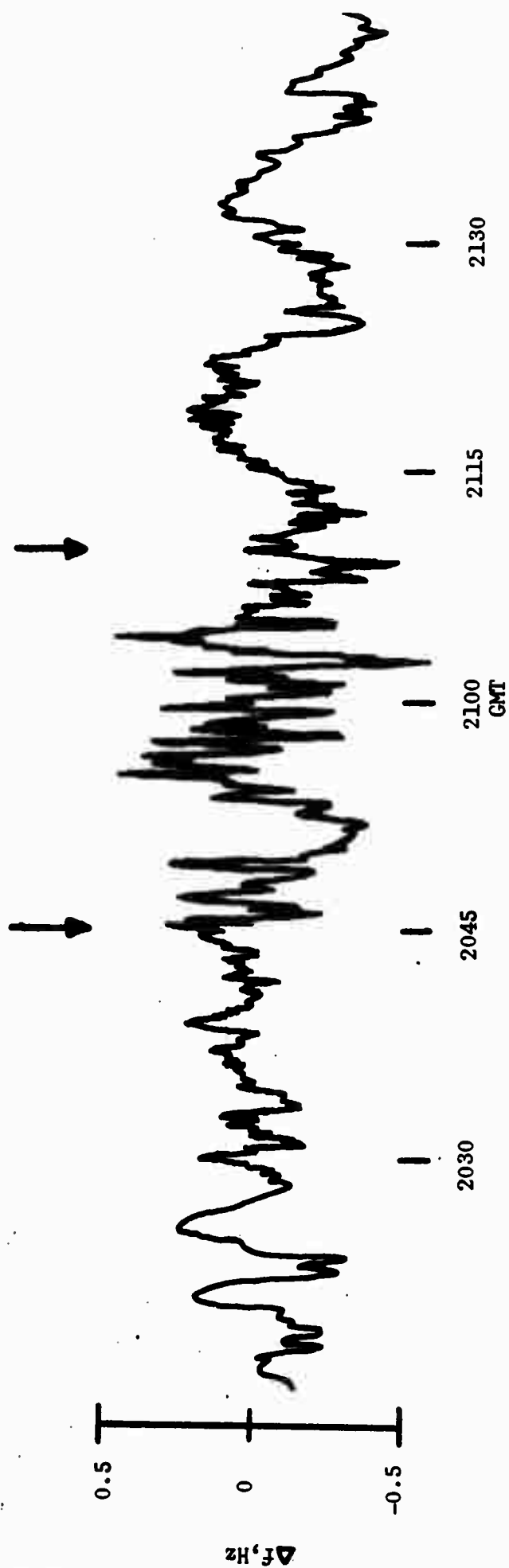
Fig. 21 4.8 MHz phase-path sounder record of May 31, 1970, following the Peruvian earthquake. Arrows indicate the time interval used for the cophase analysis in Fig. 22.
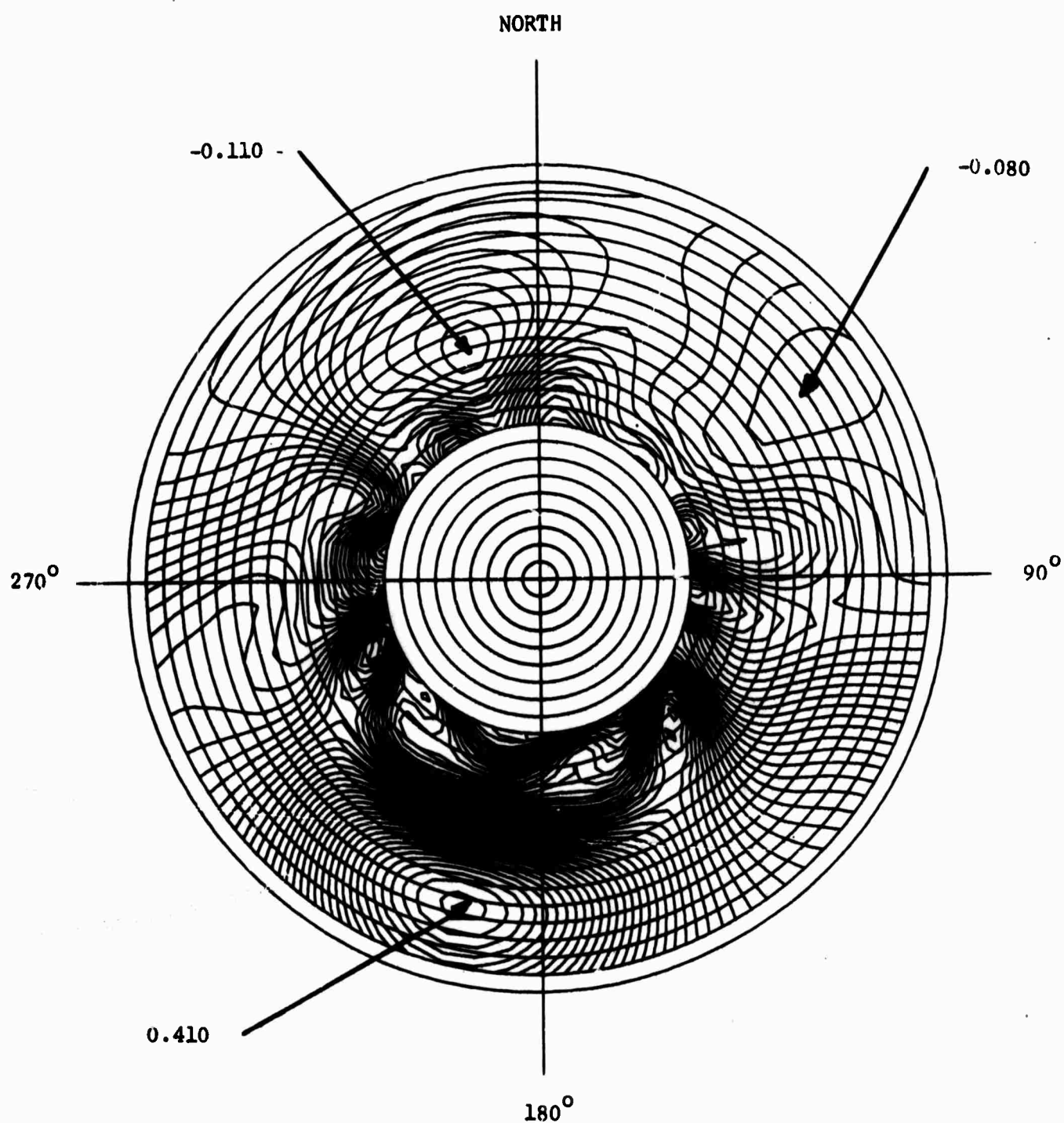
Fig 22 Cophase of the four 4.8 MHz phase-path sounder records, at the
time indicated in Fig. la. Radius is velocity, from 0 to 4800
m sec^{-1} in steps of 200 m sec^{-1}. Contour interval is 0.01.

**TELEDYNE
ISOTOPES**

corresponding to this event did not show any signal. This was expected since the displacements of the atmosphere at ground level are very small, and the resultant pressure variations were below the sensitivity of the instruments.

TELEDYNE ISOTOPES

6. SPATIAL COHERENCE OF IONOSPHERIC MOTIONS

The study of the spatial coherence, that is, the similarity of wave-forms as they propagate in space, is important because this information is vital to the design of an array as well as to the selection of the array processing techniques.

A preliminary study of this kind has been carried out. This study compares the coherencies of signals detected by the phase-path sounder array with the coherence of the background field.

6.1 Signal Coherence

Two kinds of signals have been used to investigate the spatial coherence: 1) signals generated by the Saturn-Apollo 12 rocket which cover a frequency band 0.00208Hz to 0.00832Hz (2 min – 8 min); 2) natural signals such as medium size TID's (Traveling Ionospheric Disturbances) which have a bandpass from about 0.000416Hz – 0.00139Hz (12 min – 40 min). The horizontal distance between ionospheric reflection points ranges from 63 km to 128 km.

6.1.1 Saturn-Apollo 12 Signals

The spatial coherence was obtained from the cross-spectral analyses of the various station pairs. The record length used in the analyses was 80 minutes and included the whole signal. The length of the lag window was 8 minutes. Figures 23 and 24 show some results of the cross-spectral analyses for time intervals prior to the arrival of the signal and including the signal.

Figure 25 shows the results of the coherence for the frequency bands 15, 22.5 and 30 CPH, which correspond to periods of 4, 2.667, and 2 minutes respectively. The coherence values range from 0.2 to 0.8. The average horizontal phase velocity is 720 m sec^{-1}, that is, the average wavelength is 100 km.

FIG. 23   Cross-spectrum analysis between the 4.8 MHz doppler traces of Lebanon and Thornhurst for a time   erval immediately before the arrival of signals from SATURN-APOLLO XII, showing the background noise coherence.
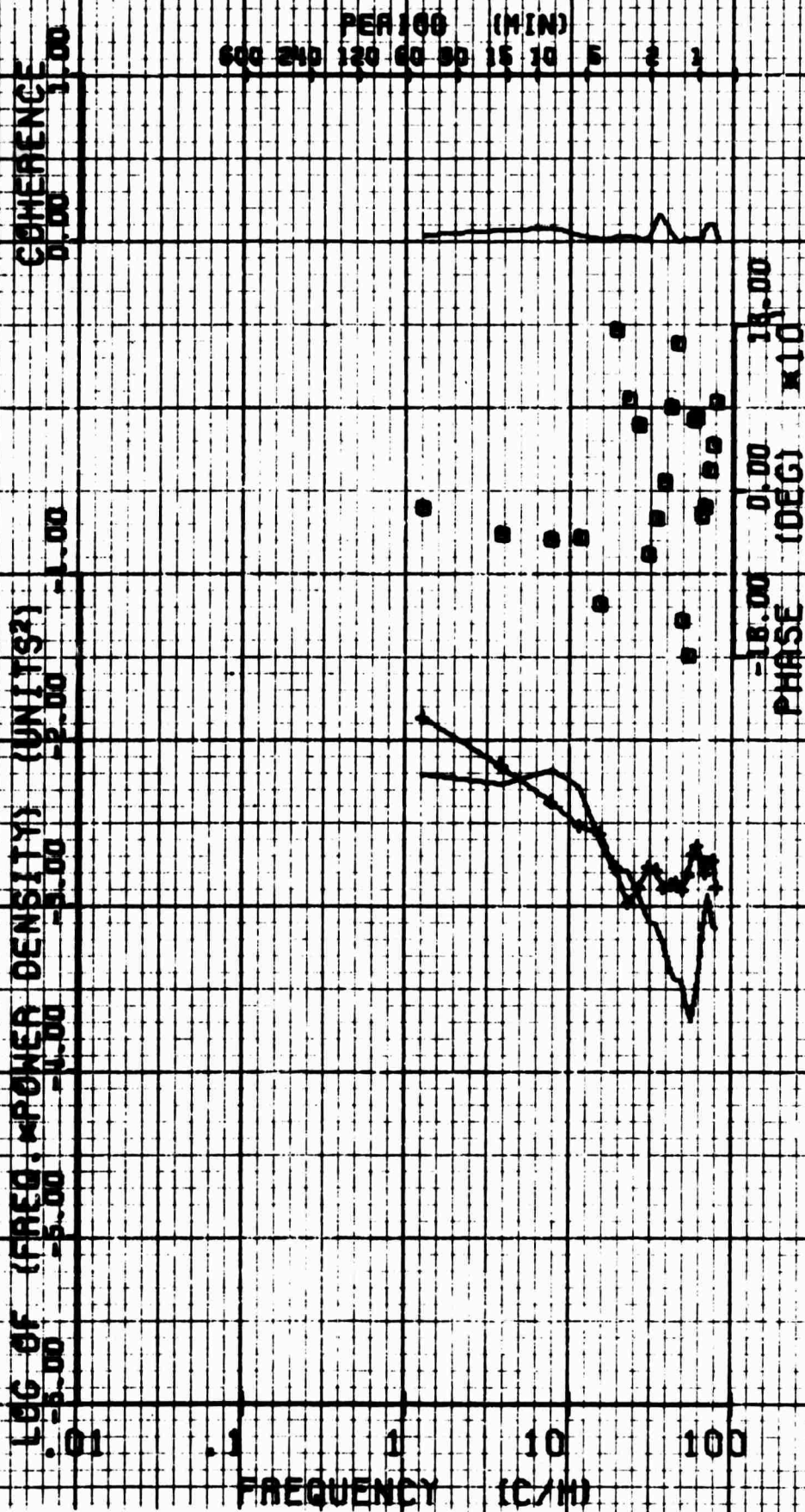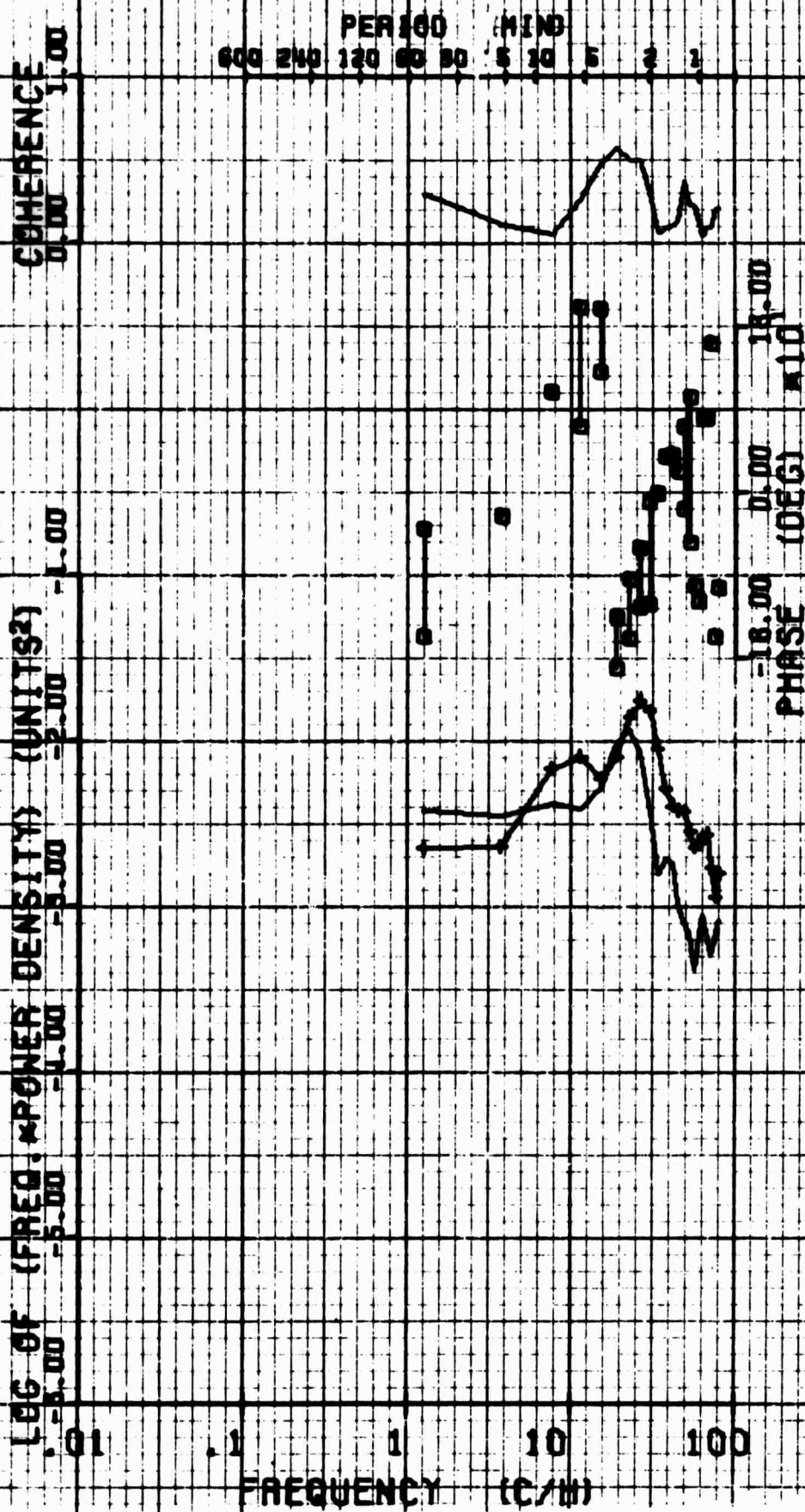
FIG. 24. Cross-spectrum analysis between the 4.8 MHz doppler traces of Lebanon and Thornhurst for a time interval including the SATURN-APOLLO XII Signal showing the spectral and coherence peaks.
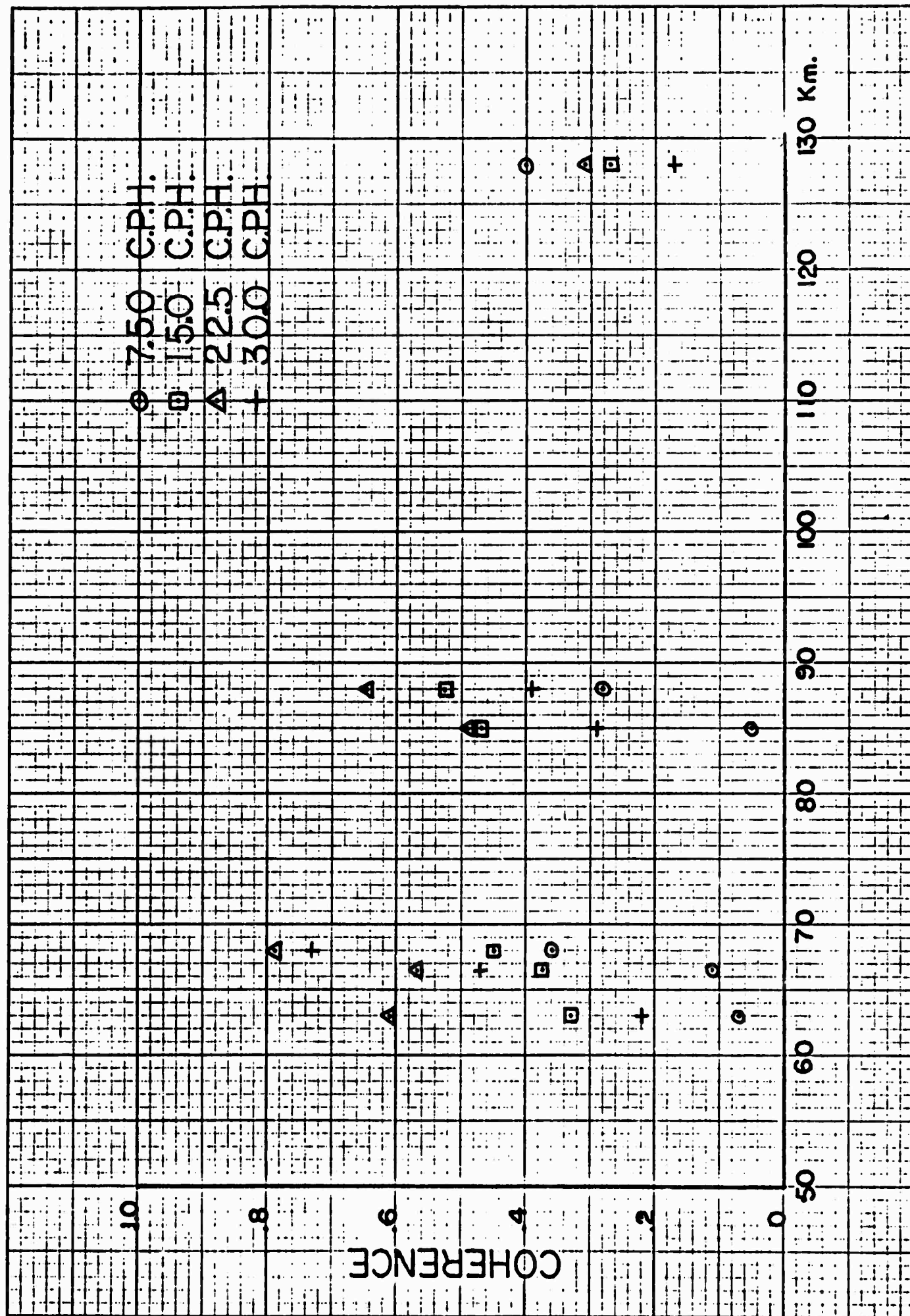
FIGURE 25   Spatial coherence for the SATURN–APOLLO XII event on 14 November 1969.

The coherence analysis indicates that the signal has suffered considerable dispersion in a distance of the order of a wavelength.

6.1.2   TID Event of 23 November 1969

In order to study the spatial coherence in the longer period ranges (18 min to 36 min) a typical TID event (**Fig. 26**) was used in the analysis. The cross-spectral analyses indicated that the energy is mainly concentrated in the frequency range 1.4 CPH to 5.0 CPH. The record length used in the analyses was the same as the duration of the event, that is, 7 hours. The coherence values for the frequency bands 1.667, 2.50 and 3.33 CPH, corresponding to periods of 36, 24 and 18 minutes respectively, have been plotted as a function of horizontal separation between reflection points along the direction of propagation (Fig. 27). It can be seen from this figure that the coherences have values of 0.5 or better up to separations between reflection points of about 80 km, decreasing for larger separations.

6.2   Background Noise Coherence

To compare the coherence of signal and noise fields, cross-spectral analyses were applied to the records corresponding to the various station pairs at time intervals during which no noticeable events occurred.

In the case of the short period ranges, records corresponding to time intervals prior to and after the arrival of the signals from the Saturn-Apollo 12 rocket were used to illustrate the background coherence. The spectral window and record length were the same as in the case of the signals. The results are shown in Figures 28 and 29 and indicate that for this period range the values of the background coherence do not exceed 0.3 at all separations.
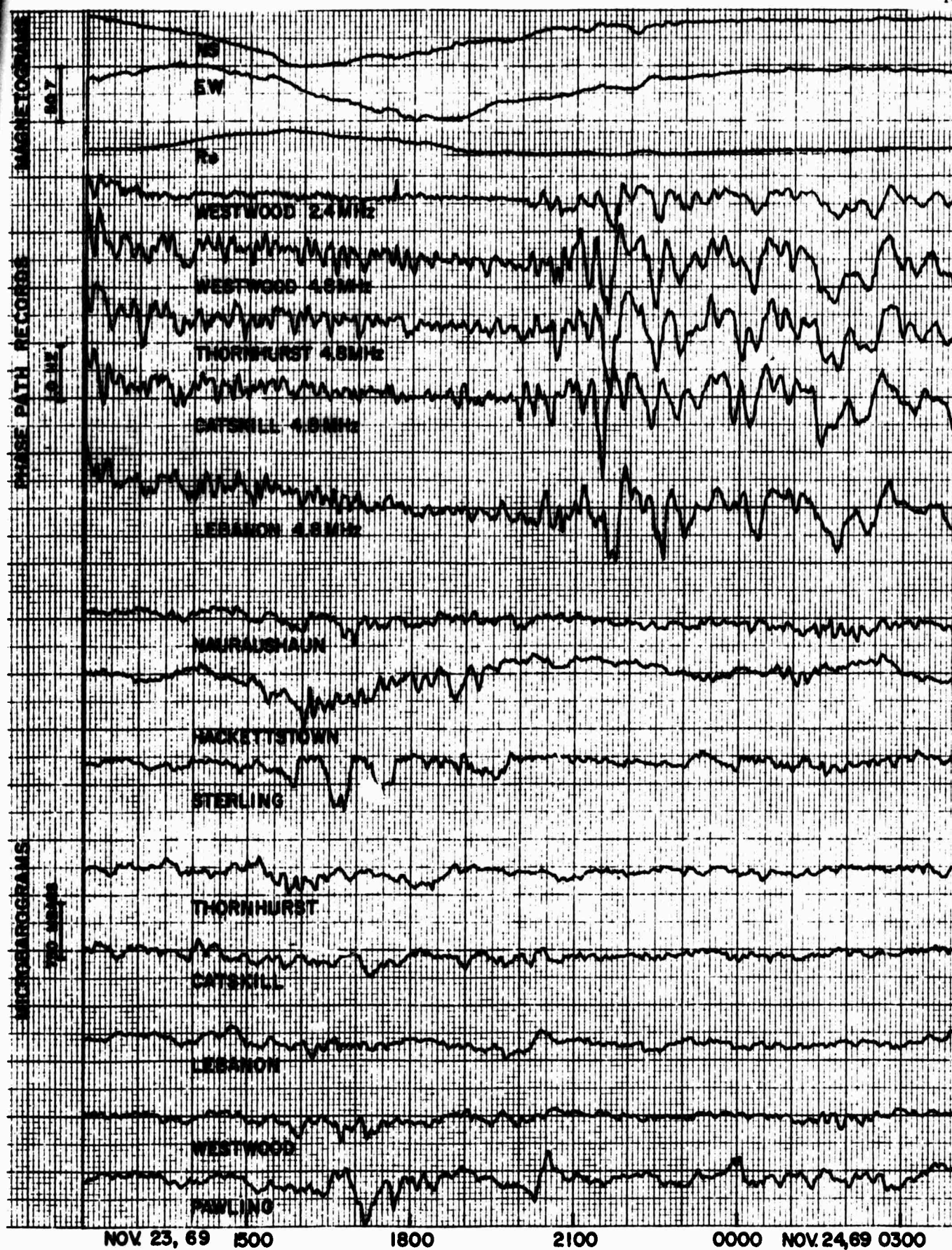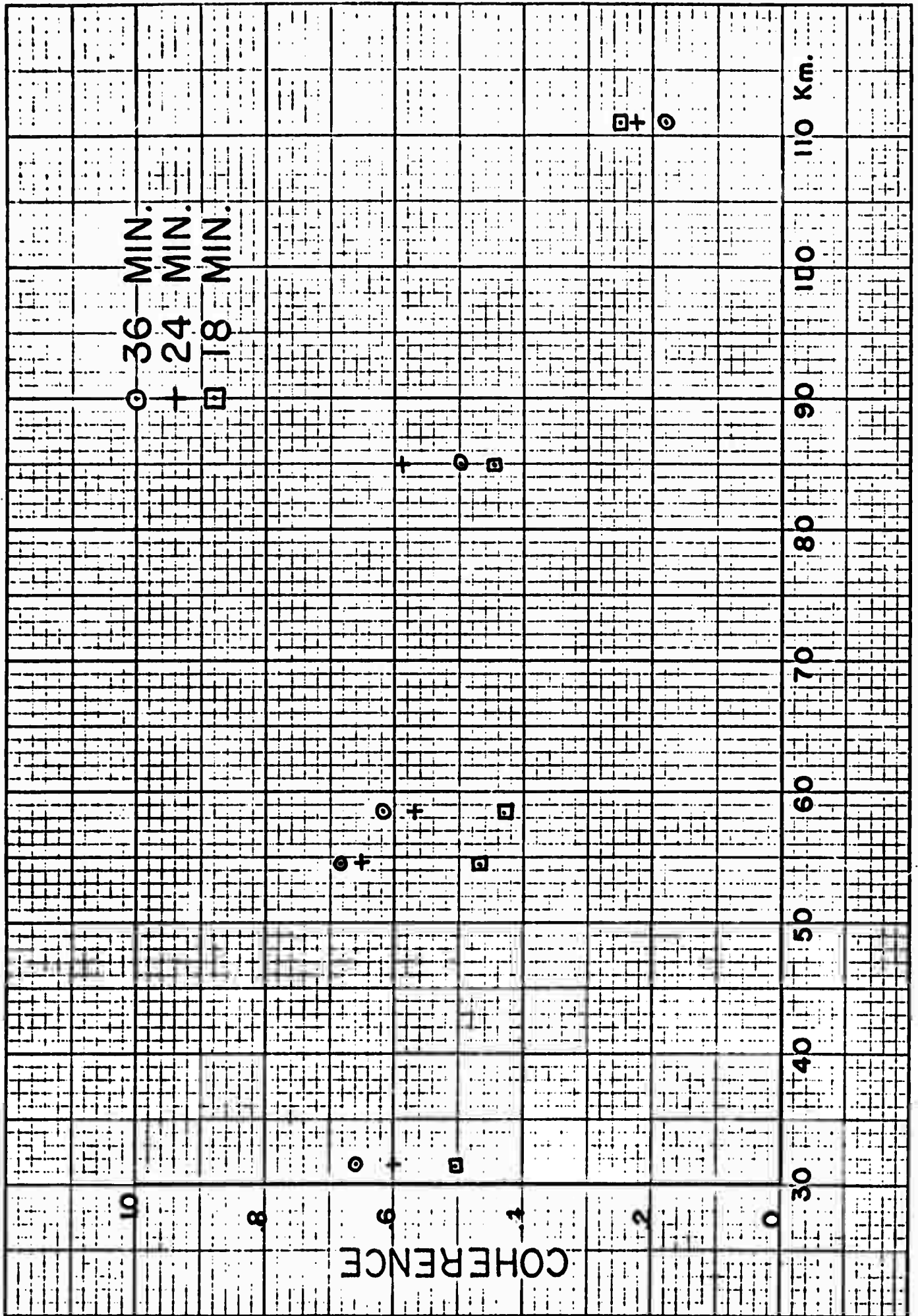
Fig. 26   TID event of November 23, 1969.

FIGURE 27   Spatial coherence for the typical TID of 23 November 1969.
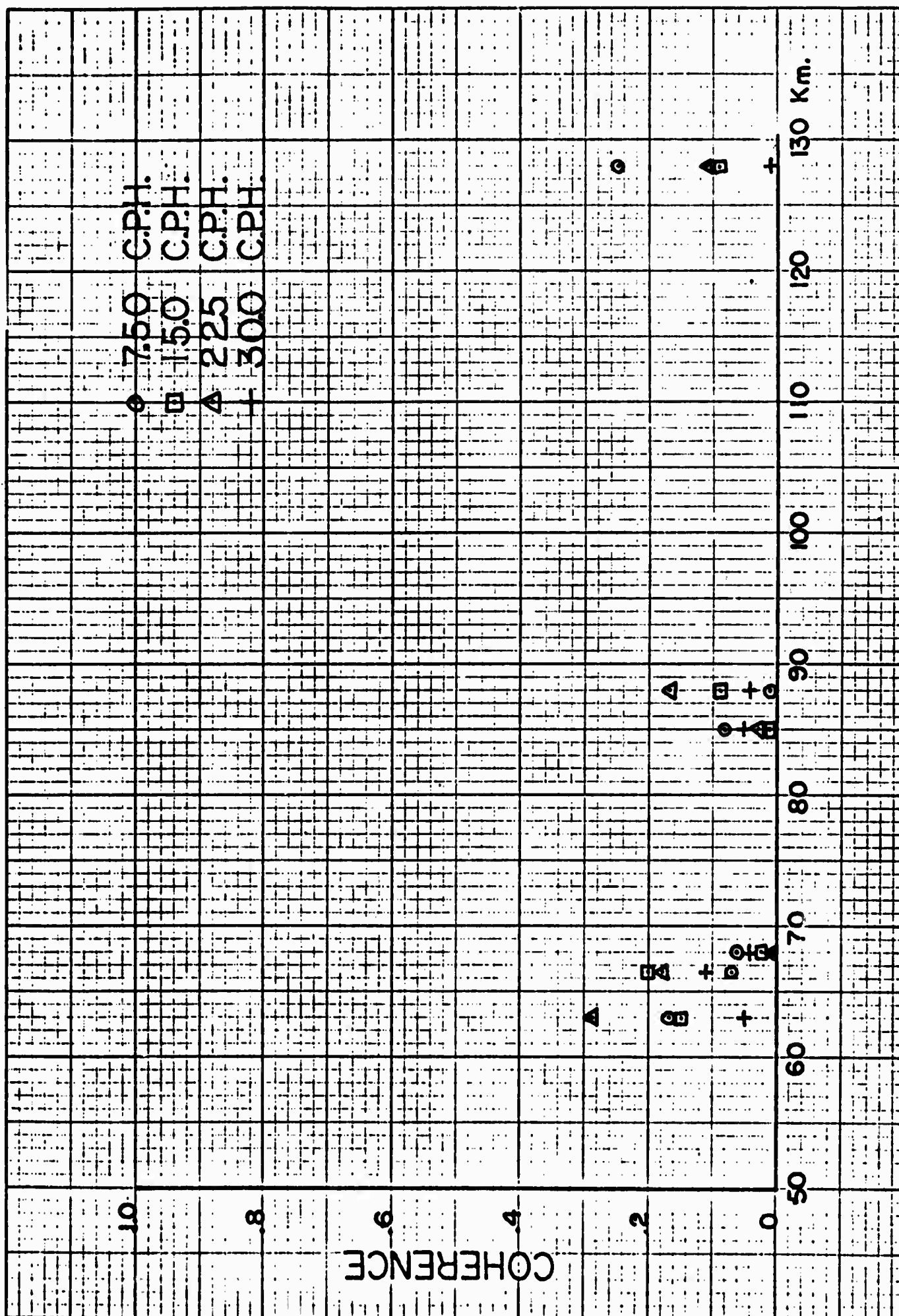
FIGURE 28   Spatial coherence for the background field prior to the arrival of the SATURN-APOLLO XII signals.

48
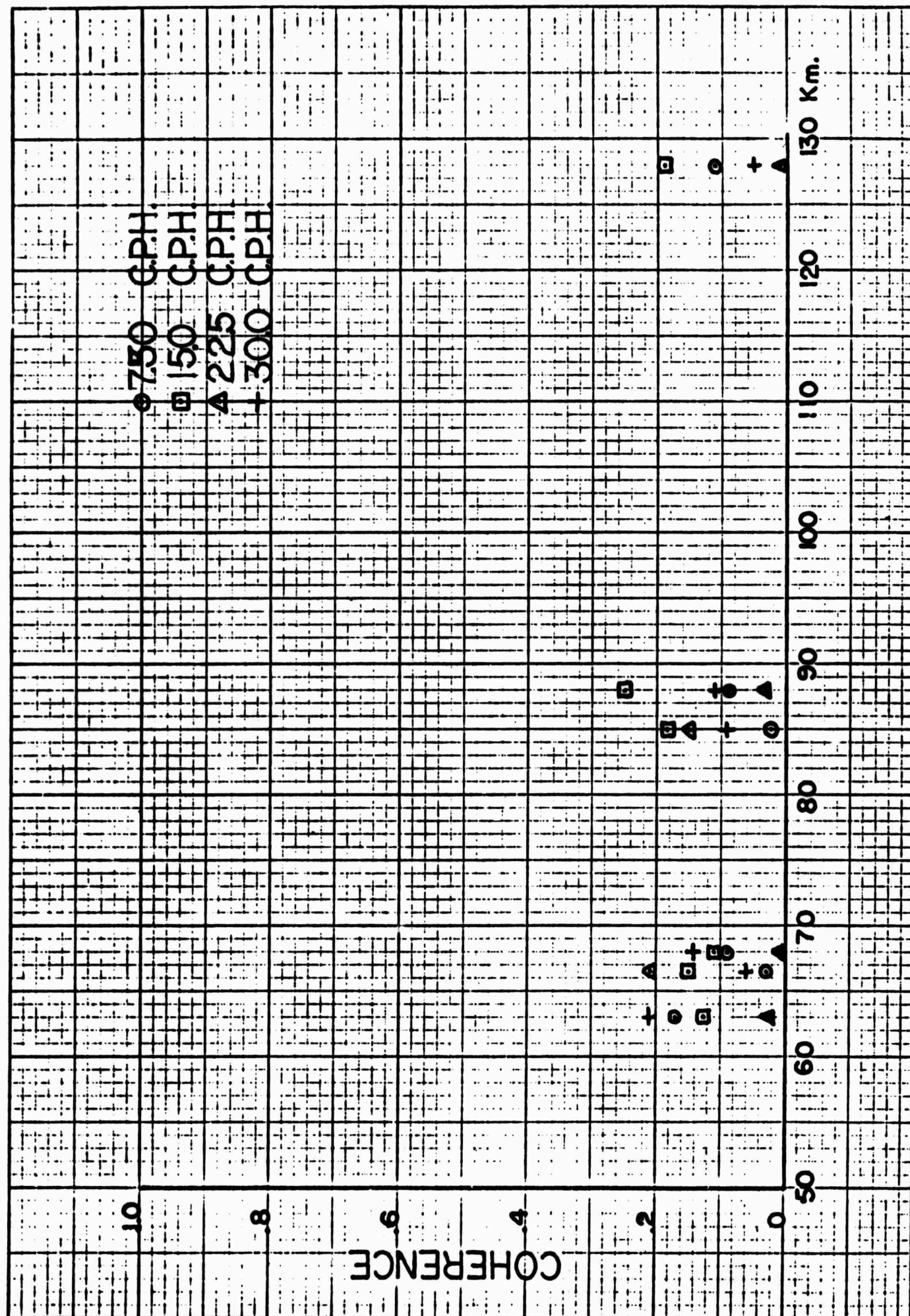
FIGURE 29 Spatial coherence for the background field after the arrival of the SATURN-APOLLO XII signals.

**TELEDYNE
ISOTOPES**

For the long period range, record lengths of 6 hours were used in the analyses. The windows were centered at 0100, 0700, 1300, and 1900 hours GMT. The results shown in Figures 30 through 33 are the average of ten days of data during the month of January 1970, and thus they are probably in some way representative of winter months. (This is, of course, subject to further analyses.) The background activity, centered at a period of 36 minutes, showed coherence values greater than 0.5 during local nighttime hours and separations between ionospheric reflection points up to 90 km, decreasing to values smaller than 0.5 during daytime hours or ionospheric reflection point separations larger than 90 km. Periods shorter than 36 minutes showed no significant change in the value of the coherence from nighttime to daytime hours. Their values were always less than 0.4.

The results of the signal and noise coherence studies indicate that in order to study short period events (periods shorter than 30 min), horizontal separations between ionospheric reflection points of the order of 60 km or so are sufficient as far as the background field is concerned since the noise in this period range is uncorrelated (low coherence) for distances of 60 km and greater. It must be pointed out that we do not know what are the characteristics of the noise for separations between reflection points shorter than 60 km since the proposed mobile receiving station was not approved.

If one desires to study longer periods (periods of the order of 30 min or longer) separations between ionospheric reflection points of about 90 to 100 km are necessary for the background noise to decorrelate.

FIGURE 90   Spatial coherence for the background field-data window corresponding to 2200Z – 0400Z.
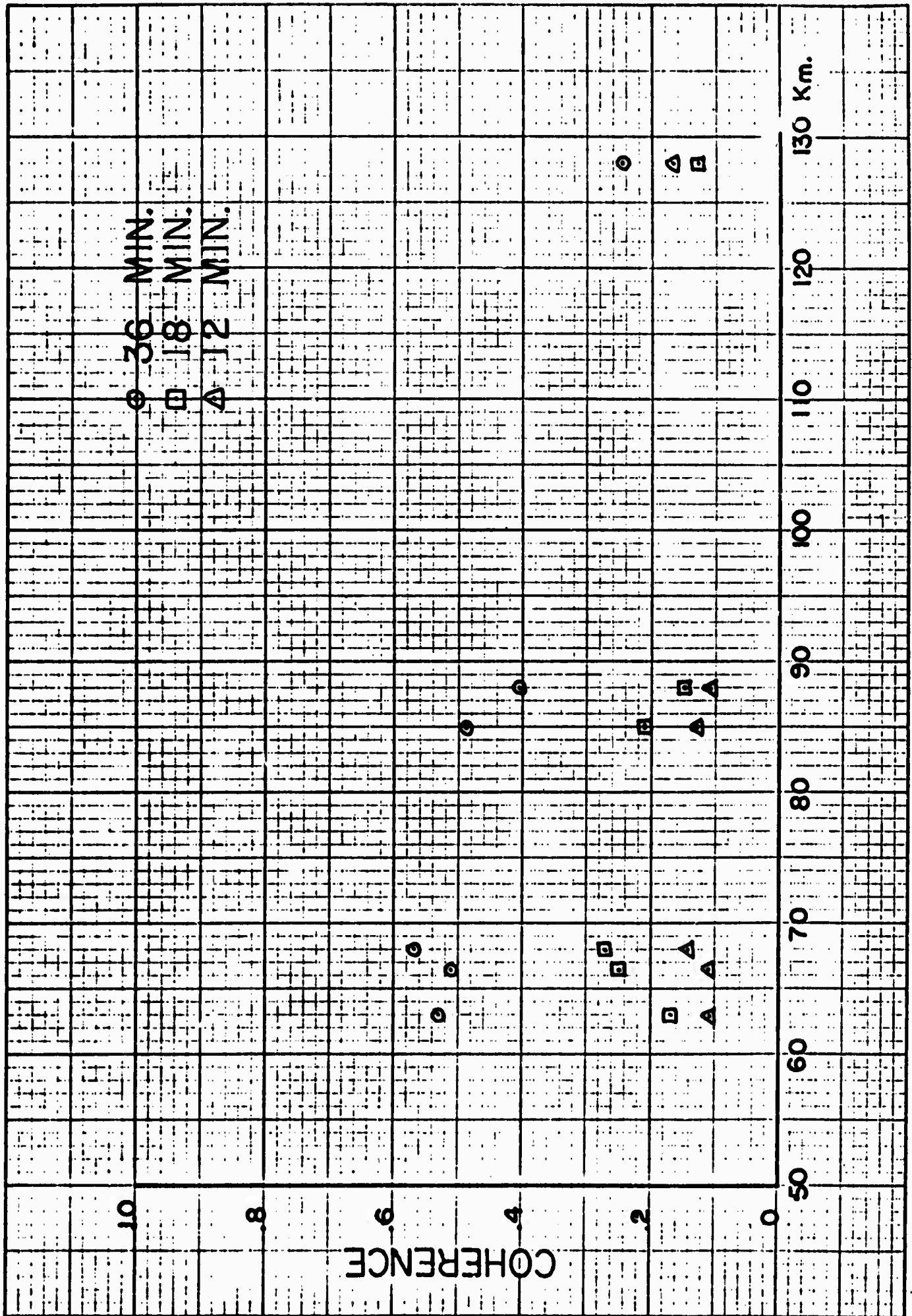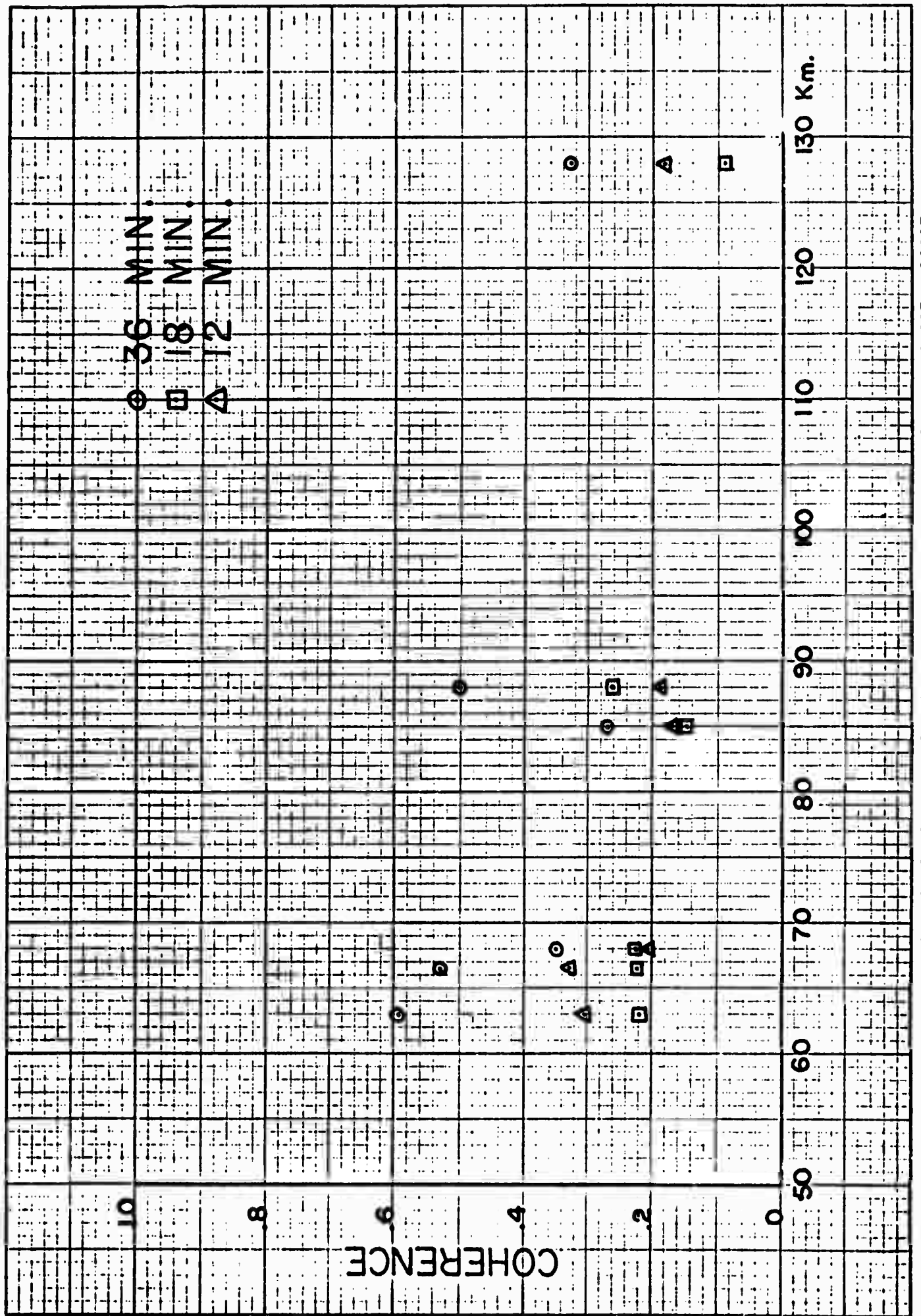
FIGURE 31   Spatial coherence for the background field. Data window corresponding to 0400Z – 1000Z.
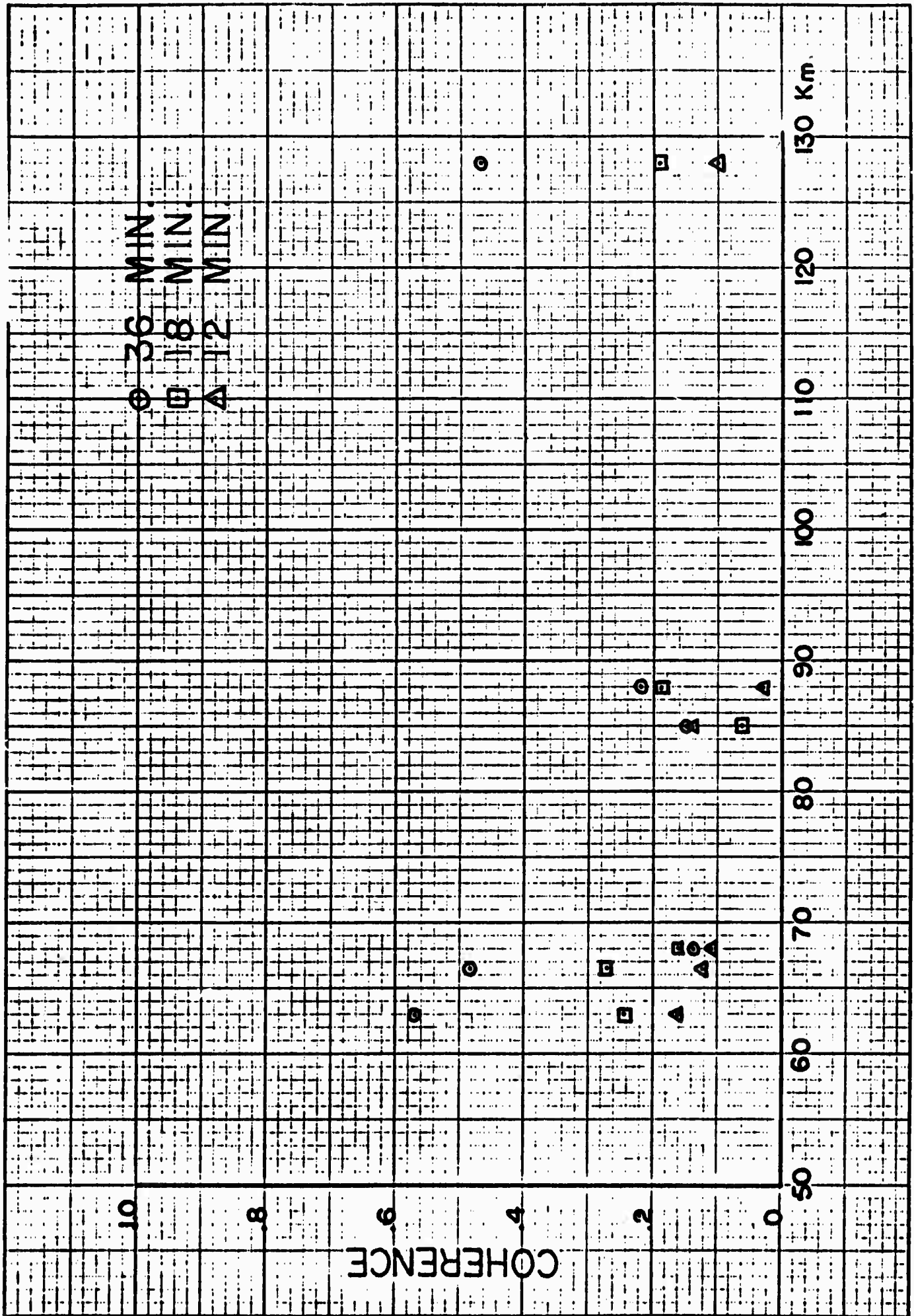
FIGURE 32   Spatial coherence for the background field.   Data window corresponding to 1000Z – 1600Z.
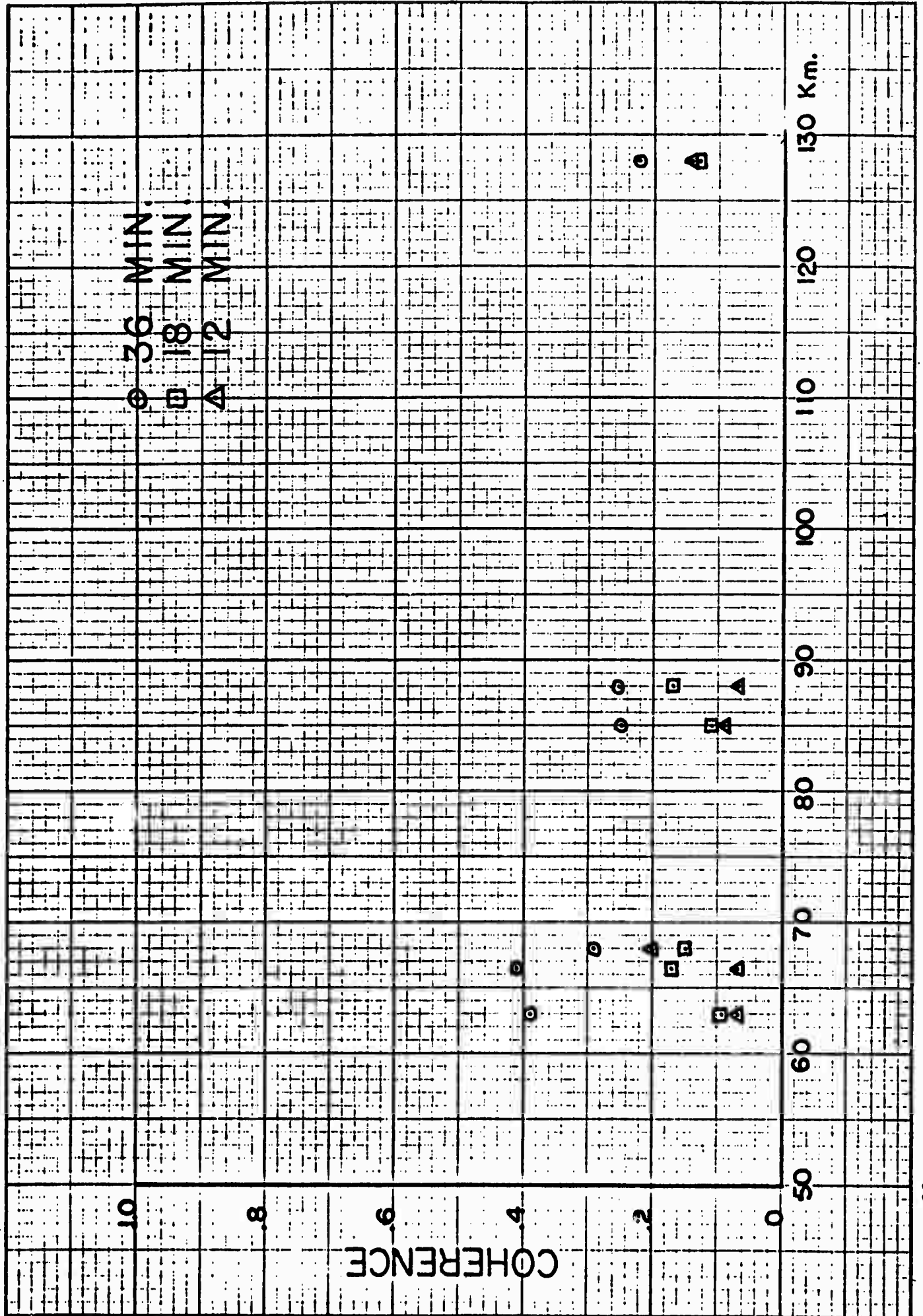
FIGURE 33   Spatial coherence for the background field.   Data window corresponding to 1600Z - 2200Z.

Long period atmospheric wave arrivals, from the nuclear tests at Mururoa Atoll, South Pacific, in 1970 were recorded by the microbarograph array. A preliminary report on these arrivals is given below.

Arrivals recorded by the phase-path sounder array will be reported later, since the conventional ionosonde data, needed for the correct interpretation of the doppler records, was not available at the time of writing this report.

The analyses of the microbarograph recordings were carried out with the cophase array processor described by Montes et al., (1970). Record samples of 60 and 80 min were used in the analyses.

Test of 30 May 1970

An arrival corresponding to the long period atmospheric wave (wavelength 400 km) was recorded by the microbarograph array. One typical microbarograph record is shown in Figure 34. The signal-to-noise ratio is too small for the signal to be visually detected. Cophase analysis was applied to the data using an 80-minute window which was shifted in time in steps of 15 minutes until a signal was "detected".

A contour plot of cophase (Fig. 35) is shown for velocities from 270 to 780 m sec^{-1} for the 80 min sample beginning at 2331Z, 30 May 1970. The distribution of cophase for random noise, evaluated at a velocity and azimuth selected a priori, is N (0,0.077) for this number of frequencies and detectors. If we expect a signal from azimuth 238° (the azimuth of Mururoa Atoll, site of the high energy event of 30 May 1970) with a phase speed of 600 m sec^{-1} (the speed associated with the long-period mode discussed by Tolstoy, 1967), its arrival is confirmed by noting that C(600,238°) is 0.345 more than four standard deviations from its expectance in the absence of signal, which
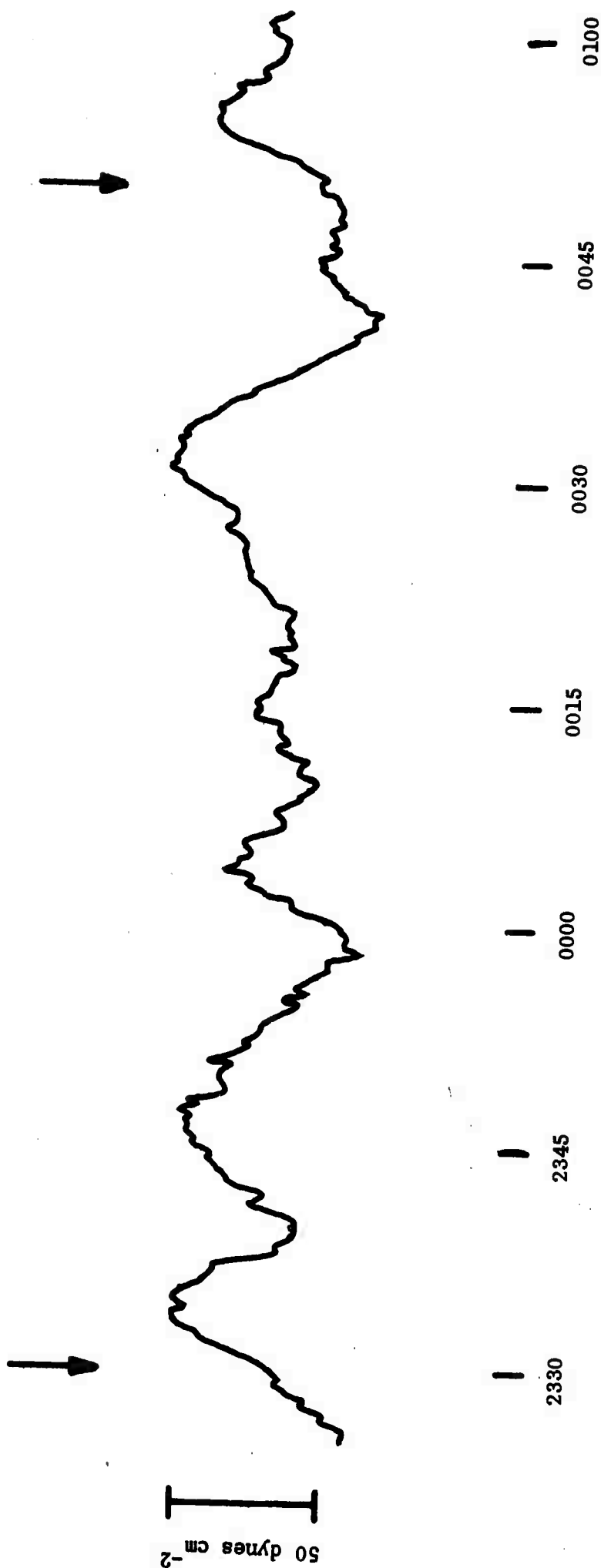
Fig. 34 Microbarograph record of May 30, 1970, following the highenergy event on Mururoa Atoll. Arrows indicate the time interval used for the cophase analysis in Fig 35.

50 dynes cm^{-2}

**TELEDYNE
ISOTOPES**

is highly significant at the 99% level. The signal has thus been "detected" by calculating its cophase at its expected speed and direction.

If the signal's presence has been assumed or detected beforehand, the maximum value of the cophase may be determined from Figure 35, and the velocity (585 m sec^{-1}) and source azimuth (245°) at that maximum, may be used as esti-mates of the corresponding signal parameters. The velocity estimate indicates that the signal detected here is of the long-period, high speed type previous-ly reported by Tolstoy and Herron (1970) and Montes et al., (1970) and discussed theoretically by Tolstoy (1967) and Tolstoy and Pan (1970). The estimate azi-muth differs by 7° from that of Mururoa Atoll. This small discrepancy is easily accounted for by the effect of winds.

Test of 3 July 1970

A similar analysis of the microbarograph records following the test of 3 July 1970 indicated that a long period signal was "detected" at 2310Z on 3 July 1970. A contour plot of cophase is shown in Figure 36. The dominant periods are between 10 - 13.3 m and the phase velocity is 540 m sec^{-1}. The azimuth of 200° differs by about 30° from the expected arrival azimuths. The cophase is C=0.400. The phase velocity indicates that this observation is also consistent with the long-period fast arrival discussed by Tolstoy. The discrepancy between observed and expected azimuths could be accounted for by strong local winds.

Tests of 15 May, 22 May, 27 July - 1970

Cophase analyses of the microbarograph records following the tests on 15 May and 22 May 1970 indicated no long period signals. The cophase analy-sis of the records corresponding to the test of 27 July 1970 gave a phase velocity of 420 m sec^{-1} and an azimuth of 225°. The value of the cophase was

NORTH

0°

-0.120

270°

90°

0.345

-0.140

180°
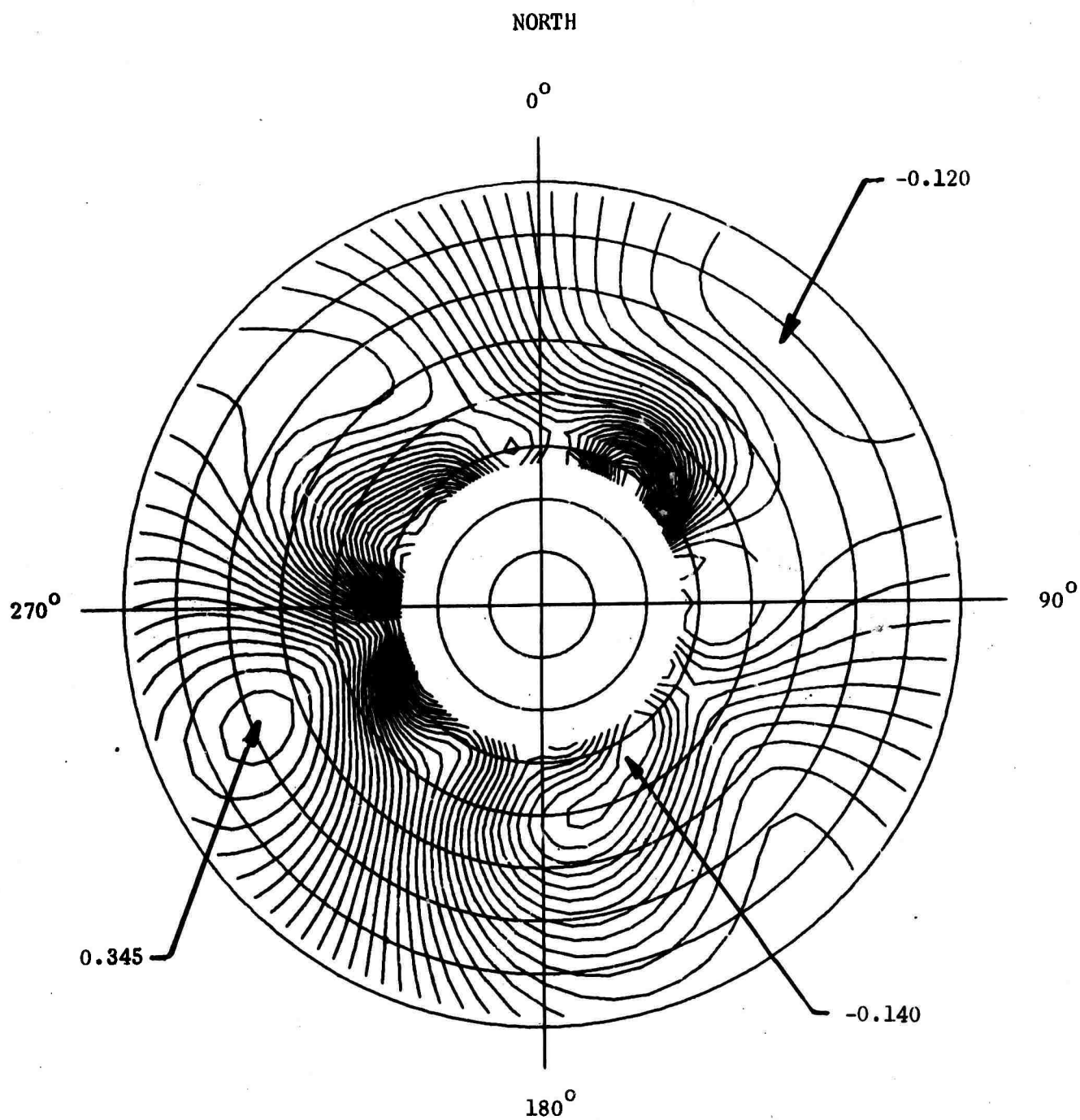
Fig. 35 Cophase of eight microbarograph records, at the time indicated
in Fig. 34. Radius is velocity, from 0 to 800 m sec^{-1} in steps
of 100 m sec^{-1}. Contour interval is 0.01.

NORTH

0°

-0.094

0.000

270°   90°

0.400

180°
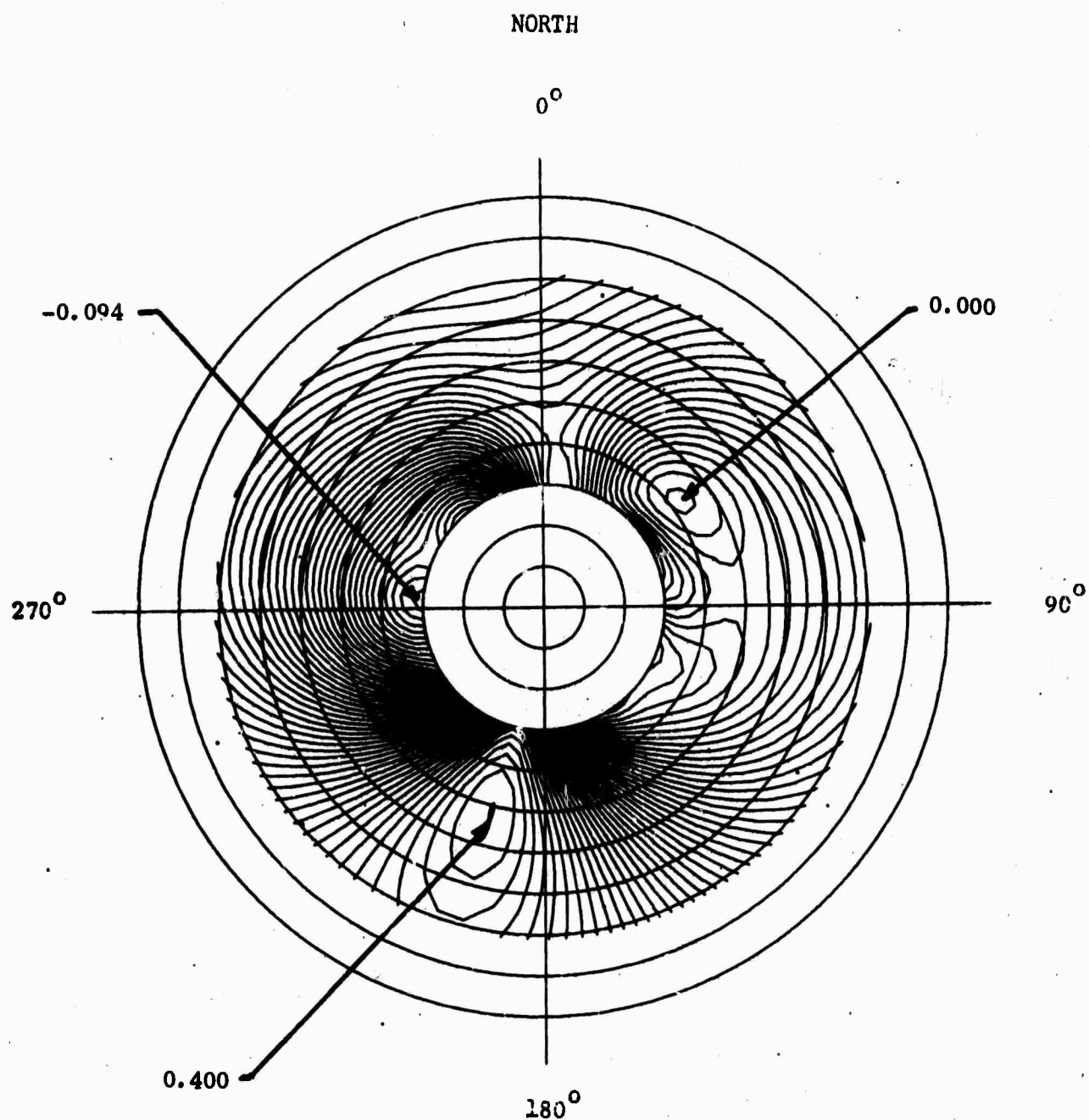
Fig. 36   Cophase of eight microbarograph records. 80 min window
            starting at 2310 Z on July 3, 1970. Radius is velocity,
            from 0 to 1000 m sec^{-1} in steps of 100 m sec^{-1}. Contour
            interval is 0.01.

TELEDYNE ISOTOPES

$C \approx 0.456$. The dominant period for this "arrival" is 10 min. The low phase velocity is not consistent with the estimated group velocity of 540 m sec^{-1}, and we will not interpret this result as an arrival from the test site until further analysis is carried out.

These preliminary results lend further support to the previous observations of the long-period mode reported by Tolstoy and Herron (1970) and Montes et al., (1970).

In the field of data processing, two developments must be reported.

8.1 Deconvolution by Directional Response of the Array

A procedure to deconvolve the function - amplitude versus direction for an actual record - by the directional response of the array was developed by Dr. Eric Posmentier. The application of this procedure removes those maxima in the function which are merely side lobes of the array response, while not affecting "real" maxima. The method begins by calculating the array's theoretical directional response to a signal from the direction of the function's extremum. (This response is the combined response over the same band of frequencies used in reducing the data to the function being deconvolved.) A fixed arbitrary fraction (usually 0.1) of this response, multiplied by the function's value at the extremum, is subtracted from the original function, resulting in a residual function. This is reiterated until the RMS value of the residual function falls below a predetermined value. The total of the amplitudes of the signals centered at each direction and subtracted from successive residual functions represents the desired deconvolution.

A computer program to apply this concept to actual array data has been written in Fortran IV for the IBM 360/44.

8.2 True-Height Analysis of Ionograms

In order to relate the doppler observations to heights of reflection in the ionosphere it is necessary to reduce conventional ionosonde data or ionograms to true-height. A computer program to perform this conversion was adapted to work on our computer. The program is based on the polynomial analysis of Titheridge (1967). The original program which was written in BASIC language was made available by Dr. Carlos Calderon from Dartmouth College.

8.3 Parameter Estimation for an R-Dimensional Plane Wave

A Theoretical study of the parameter estimation of an R-dimensional plane wave has been carried out in cooperation with Dr. M. Hinich of Carnegie-Mellon University. This study is relevant to the extension of the delay and sum beamforming technique to the case in which the wave parameters are measured in three dimensions such as the case of a multifrequency phase-path sounder array. This work has been submitted for publication to the Annals of Mathematical Statistics under the title: "Parameter Estimation for an R-Dimensional Plane Wave Observed with Additive Independent Gaussian Errors".

The accomplishments of the research effort during the period 1 October
1969 to 30 September 1970 can be summarized as follows.

1. The existing 4-element phase-path (doppler) sounder array has been
expanded to operate with two sounding frequencies simultaneously. The
sounding frequencies allocated by the FCC were 4.824 MHz and 6.030 MHz.
The radio reflection levels for these frequencies range from 150 to
300 km. This expanded array has been in operation in conjunction with
the microbarograph and magnetometer arrays (Montes, et al., 1970) from
April 1970 through September 30, 1970.

Calculations were undertaken to find the theoretical amplitude
response for the doppler array as function of wavelength and azimuth.
These calculations showed the existence of many side lobes for wave-
lengths of the order of 40 km. The size of the side lobes decreased for
azimuths near $0°$ and $180°$; that is, for NS propagation. At 80 km wave-
length the side lobes still persist but the main lobe stands out clearly.
For wavelengths of about 120 km there is a large side lobe probably pro-
duced by a ringing effect in space. At larger wavelengths the side lobes
are small, and identification of the main lobe is straightforward. The
addition of one or two more elements (in the EW direction) would greatly
improve the response of the array in this direction. It should be
pointed out that the present arrangement for the doppler array was one
of the best one could obtain with 4 elements and being restricted to
occupying any of the existing microbarograph stations.

2. The study of ionospheric background motions, initiated last year, was continued during this contract period, producing important results.

It has been found that the power spectra of the phase-path variations show the effect of a varying Väisälä frequency with height, probably modified by the effects of viscosity. Although at this stage it is not possible to offer a quantitative theory of the power spectrum behavior, some points appear suggestive.

a) The fact that the power spectrum peaks and slope breaks tend to follow the calculated $N(z)$ curves cannot be explained solely in terms of viscosity.

b) The appearance itself of power spectrum peaks for $\omega = N$ is difficult to explain by the effect of viscosity alone, since this would require a generating process with a spectrum having the unlikely property of rising steeply towards the higher frequencies before being knocked down and filtered out by viscosity.

c) The appearance of breaks in the power spectrum slopes is more suggestive of a frequency cutoff effect than of increasing viscous damping.

It appears therefore that the peak frequencies and slope break frequencies measured on the phase-path fluctuation power spectra are representative of the local values of the Väisälä frequency $N(z)$. Inclusion of viscosity into the theory of gravity wave propagation would permit a quantitative interpretation of the spectra making it possible to derive the parameters of the neutral gas structure, at ionospheric levels, from observations of this type.

TELEDYNE ISOTOPES

3. A study of phase-path records following the Saturn-Apollo launches indicates that rocket-generated infrasound is trapped at ionospheric heights. The group velocity of 450 m sec^{-1} suggests a ducting mechanism in which waves are totally reflected at the top of the wave guide by the increasing sound speed and almost totally reflected at the bottom from the mesosphere by the increase of the acoustic cut-off frequency. More sophisticated atmospheric models to fit these observations could provide important neutral structure data.

4. Array processing of the phase-path (doppler) records following the Peruvian earthquake of 31 May 1970 indicated the presence of signals with periods between 0.3 and 3.0 min. The arrival azimuth and horizontal phase velocity of these signals were 190° $\pm$ 5° and 3.9 km sec^{-1} respectively. Although arrivals of this kind have been previously reported and explained by other workers as the coupling between seismic Rayleigh waves and atmospheric waves, our observation is the first one in which the azimuth and phase velocity have been measured. These wave parameters are two of the <u>most important evidences</u> of coupling between seismic surface waves and atmospheric waves.

5. Investigations of the spatial coherence of ionospheric motions were carried out using phase-path records corresponding to the Saturn-Apollo 12 event and a TID event. These studies indicate that horizontal separations between ionospheric reflection points of the order of 60 km or so are sufficient, for noise decorrelation, when studying events whose periods are shorter than 30 min. Longer periods require separations of the order of 90 to 100 km for effective background noise decorrelation.

**TELEDYNE
ISOTOPES**

6. Preliminary analyses of the microbarograph records following the nuclear tests at Muroroa Atoll on 30 May and 3 July 1970 indicated the arrival of long period waves (T > 10 min) from the direction of the test site. Array processing of these events gave phase velocities of 585 m sec^{-1} for the 30 May event and 540 m sec^{-1} for the 3 July event. No arrivals were found following the tests on 15 May and 22 May, 1970.

The wave parameters of the observed arrivals are similar to those reported by Tolstoy and Herron (1970) and Montes, et al., (1970), lending further support to these previous observations.

7. In the theoretical aspect of data processing, two studies have been completed:

a) A procedure and the corresponding computer software to deconvolve the function-amplitude versus direction for an actual record,

b) A theoretical study of the parameter estimation for an R-dimensional plane wave. This study is relevant to the extension of the delay and sum beam steering technique to the analysis of data from a three dimensional array such as the doppler array.

To conclude we wish to point out that during the experimental phase of this project it has been possible to accumulate a unique collection of digital data corresponding to simultaneous measurements of ionospheric motions, pressure variations and geomagnetic fluctuations. In order to extract the potential of these previous observations, it is necessary to subject to data to considerable further study, in particular, the following points should be thoroughly investigated.

TELEDYNE
ISOTOPES

a) Analyses of data corresponding to nuclear events with respect to doppler-microbarograph correlations and determination of all the circumstances under which simultaneous recordings can be made on both arrays.

b) Dispersion analyses of TID's observed in the doppler records in order to secure structural data of the neutral gas at upper atmospheric levels. Structural information, and in particular, estimates of the Väisälä frequency and acoustic cutoff frequencies are vital to the diagnostic use of arrivals from nuclear explosions (Tolstoy and Pan, 1970). These dispersion studies are the most economic means of securing this type of information.

c) Analyses of Saturn-Apollo generated signals observed on doppler records for the purpose of obtaining structure information in the region 100-250 km where these signals appear to be trapped.

d) Investigation of the doppler records with relation to several missile launches of various types to determine under which conditions of power and/or trajectory acoustic energy propagates at thermospheric levels.

1. Montes, H., C. Grosch, M. Hinich and E. Posmentier, 1970: Summary
    Report, Atmospheric Propagation Studies up to 30 September 1969.
    Teledyne Isotopes Technical Report IWL-7556-175.

2. Willis, E., H. Montes and G. Rao, 1970: Potential of Phase-path
    Sounders to Detect Atmospheric Acoustic-Gravity Waves Generated by
    Nuclear Detonations. ARPA-AFOSR Symposium report, Spring 1970.

3. Tolstoy, I., H. Montes, G. Rao and E. Willis, 1970: Long period sound
    waves in the thermosphere from Apollo launches, J. Geophys. Res., 75,
    28, 5621-5625.

4. Rao, G. L., 1970: Investigations on Travelling Ionospheric
    Disturbances (TLD) by CW Doppler (phase-path) Array. Teledyne
    Isotopes Technical Report IWL-7556-219.

1. PHASE HEIGHT FLUCTUATIONS IN THE IONOSPHERE BETWEEN 130 AND 250 KM.

I. Tolstoy and H. Montes

Power spectra of CW phase-path sounders operating at 6.0, 4.8 and 2.4 MHz often display peak or slope changes at periods in the 5 - 15 minute range. Plots of these periods vs. real height tend to follow mean Väisälä frequency curves calculated from Standard Atmosphere models. This suggests that statistical properties of CW phase-path sounder fluctuation can be used to monitor certain mean physical parameters of the upper atmosphere.

2. COPHASE: AN AD HOC ARRAY PROCESSOR

Eric S. Posmentier and Rudolph W. Herrmann

An ad hoc statistic, Cophase, is introduced for use in processing data from an array of detectors sensing both a propagating signal and un-correlated noise. Cophase is basically the normalized sum over all detector pairs, and over all frequencies, of the cosines of the differ-ences between phase differences from Fourier analysis and phase differ-ences from an assumed wave vector. The distribution of the Cophase is calculated for various signal-to-noise ratios, including zero. Several numerical experiments with synthetic signals and noise, as well as with real data presented elsewhere, show that Cophase analysis is a rapid

method of detecting signals above one-fourth the noise power, and of estimating signal phase velocity and direction. The most important limitations of the method are the intrinsic limitations of the array size and pattern, and of the signal duration and bandwidth, but not of the Cophase analysis _per se_.

3. PARAMETER ESTIMATION FOR AN R-DIMENSIONAL PLANE WAVE OBSERVED WITH ADDITIVE INDEPENDENT GAUSSIAN ERRORS

Melvin J. Hinich and Paul Shaman

Annals of Mathematical Statistics, 1971

Let $\epsilon(t,x)$ denote a stationary Gaussian process with $E\,\epsilon(t,x) = 0$, $E\,\epsilon^2(t,x) = \sigma^2$ $\forall t \epsilon \tau$, $x \epsilon \chi$, and $E\,\epsilon(t_1,x_1)\,\epsilon(t_2,x_2) = 0$ $\forall t_1 \neq t_2$ or $x_1 \neq x_2$. Let τ be the set of integers and χ a subset of the r-dimensional Euclidean space R^r. Given a coordinate system in R^r and a time origin, observe $y(t,x) = s(t,x) + \epsilon(t,x)$, where $s(t,x) = \tfrac{1}{2}a(0)$

$+\sum_{j=1}^{\frac{1}{2}(T-1)} [a(\omega_j)\cos(\omega_j t - \underset{\sim}{K}(\omega_j)'x) + b(\omega_j)\sin(\omega_j t - \underset{\sim}{K}(\omega_j)'x)]$,

$\omega_j = 2\pi j/T$, $j=1,\ldots,\tfrac{1}{2}(T-1)$ (T odd), and $\underset{\sim}{K}(\omega_j)$ is a vector of parameters in R^r. If $\underset{\sim}{K}(\omega) = (\omega/v)\,\underset{\sim}{e}$, where $\underset{\sim}{e}'\underset{\sim}{e} = 1$, $s(t,x)$ is the r-dimensional generalization of a (discrete time) plane wave which is propagating with phase velocity v in a direction parallel to $\underset{\sim}{e}$. For a finite time let the process $y(t,x)$ be simultaneously observed at each $x \epsilon \chi = S_1 \times S_2 \times \cdots \times S_r$, $S_j = (1,2,\ldots,n)$.

The periodogram (approximate maximum likelihood) estimators $\hat{a}(\omega_j)$, $\hat{b}(\omega_j)$, $\hat{\underline{\chi}}(\omega_j)$ of $a(\omega_j)$, $b(\omega_j)$, $\underline{\chi}(\omega_j)$, respectively, have a joint limiting normal distribution in which appropriately normalized estimators of the r components of $\underline{\chi}(\omega_j)$ are mutually independent, for each $j=1,\ldots,\frac{1}{2}(T-1)$. The distributions of the estimators for different ω_j's are mutually independent. The analysis is generalized to the case where $s(t,\underline{x})$ is a sum of plane waves with separation between the phase velocities.

REFERENCES

Booker, J.R. and R.P. Bretherton, 1967: The critical layer for internal gravity waves in a shear flow. J. Fluid Mech., 27, 513-539.

Davies, K. and D.M. Baker, 1965: Ionospheric effects observed around the time of the Alaskan earthquake of March 28, 1964., J. Geophys. Res. 70, 2251-2253.

Dessler, A.J., 1959: Ionospheric heating by hydromagnetic waves., J. Geophys. Res. 64, 397-401.

Donn, W., and E. Posmentier, 1964: Ground coupled air waves from the great Alaskan earthquake., J. Geophys. Res., 69, 5357.

Georges, T.M., 1967: Evidence for the influence of atmospheric waves on ionospheric motions, J. Geophys. Res. 72, 422-425.

Georges, T.M., 1968: HF Doppler studies of traveling ionospheric disturbances, J. Atmosph. Terr. Phys. 30, 735-746.

Gossard, E.E., 1962: Vertical flux of energy into the lower ionosphere from internal gravity waves generated in the troposphere, J. Geophys. Res., 67, 745.

Harkrider, D.G. and F.J. Wells, 1968: Excitation and dispersion of the atmosphere surface wave. Acoustic-gravity waves in the ionosphere symposium proceedings, 299-313.

Hines, C.O., 1960: Internal atmospheric gravity waves at ionospheric heights, Can J. Phys. 38, 1441-1481.

Hines, C.O. and C.A. Reddy, 1967: On the propagation of atmospheric gravity waves through regions of wind shear, J. Geophys. Res. 72, 1015-1034.

Hooke, W.H., 1968: Ionospheric irregularities produced by internal atmospheric gravity waves, J. Atmosph. Terr. Phys. 30, 795-823.

Jardetsky, W., and F. Press., 1952: Rayleigh-wave coupling to atmospheric compression waves, Bull. Seismol. Soc. Am., 42, 135.

Maeda, K. and T. Watanabe, 1964: Pulsating aurorae and infrasonic waves in the
      polar atmosphere. J. Atmos. Sci., 21, 15-29.

MacKinnon, R.F., 1969: Atmospheric vertical energy flux due to a ground dis-
      turbance. Can J. of Phys., 47, 707-725.

Midgeley, J.E. and H.B. Liemohn, 1966: Gravity waves in a realistic atmosphere.
      G. Geophys. Res., 71, 3729-3748.

Montes, H., C. Grosh, M. Hinich and E. Posmentier, 1970: Summary report,
      atmospheric propagation studies up to 30 September 1969. Teledyne Isotopes
      Technical Report IWL - 7556-175.

Oliver, J., 1962: A summary of observed seismic surface wave dispersion, Bull.
      Seismol. Soc. Am., 52, 81.

Phillips, O.M., 1966: The dynamics of the upper ocean. Cambridge University Press.

Pitteway, M.L.V. and C.O. Hines, 1963: The viscous damping of a atmospheric
      gravity waves. Can. J. Phys. 41, 1935-1948.

Pochapsky, T.E., 1968: Oceanic current and temperature gradients at 12 degrees N.,
      27 degrees W. J. Geophys. Res. 43, 1221.

Titheridge, J.E., 1967: The overlapping-polynomial analysis of ionograms.
      Radio Science, 2, 1165-1175.

Titheridge, J.E., 1968: Periodic disturbances in the ionosphere. J. Geophys.
      Res. 73, 243-252.

Tolstoy, I., 1963: The theory of waves in stratified fluids including the effects
      of gravity and rotation. Rev. Mod. Phys. 35, 207-230.

Tolstoy, I., 1967: Long period gravity waves in the atmosphere. J. Geophys.
      Res. 72, 4605-4622.

Tolstoy, I. and T.J. Herron, 1969: A model for atmospheric pressure fluctuations
      in the mesoscale range. J. Atmos. Sci. 26, 270-273.

TELEDYNE ISOTOPES

Tolstoy, I., and T.J. Herron, 1970: Atmospheric gravity waves from nuclear explosions, J. Atmos. Sci., 27, 55.

Tolstoy, I and P. Pan, 1970: Simplified atmospheric models and the properties of long period internal and surface gravity waves. J. Atmos. Sci. 27, 31-50.

Tolstoy, I., H. Montes, G. Rao and E. Willis, 1970: Long period sound waves in the thermosphere from Apollo launches, J. Geophys. Res., 75, 5621.

U.S. Committe on Extension to the Standard Atmosphere, 1966: U.S. Standard Atmosphere Suppliments, Government printing office, Washington, D.C.

Weaver, P., P. Yuen and G. Ploss, 1970: Acoustic coupling into the ionosphere from seismic waves of earthquake at Kurile Islands on August 11, 1969, Nature, 226, 1239.

Witt, G., 1962: Height, structure and displacements of noctilucent clouds. Tellus, 14, 1-18.